CHALMERS

Road surface estimation

Exploring road surface estimation as a part of condition monitoring

Bachelor's thesis in Mechatronics

Nils Twedmark
Victor Carlberg Dahl

DEPARTMENT OF MECHANICS AND MARITIME SCIENCES

CHALMERS UNIVERSITY OF TECHNOLOGY
Gothenburg, Sweden 2021
www.chalmers.se

Bachelor's thesis 2021:03

Road surface estimation

Exploring road surface estimation as a part of condition monitoring

Nils Twedmark
Victor Carlberg Dahl

CHALMERS

Department of Mechanics and Maritime Sciences
Chalmers University of Technology
Gothenburg, Sweden 2021

Road surface estimation
Exploring road surface estimation as a part of condition monitoring
Nils Twedmark
Victor Carlberg Dahl

Supervisor: Matthijs Klomp, Volvo Car Corporation Torslanda
Examiner: Fredrik Bruzelius, Department of Mechanics and Maritime Sciences

Bachelor's Thesis 2021:03
Department of Mechanics and Maritime Sciences
Chalmers University of Technology
SE-412 96 Gothenburg
Telephone +46 31 772 1000

Cover: The car used for testing.

Typeset in LaTeX
Printed by Chalmers Reproservice
Gothenburg, Sweden 2021

Road surface estimation
Exploring road surface estimation as a part of condition monitoring
Nils Twedmark
Victor Carlberg Dahl
Department of Mechanics and Maritime Sciences
Chalmers University of Technology

Abstract

This thesis explored if it is possible to estimate road surface by measuring the acceleration of the vehicle's suspension, sprung and unsprung mass. Being able to estimate the road surface can be advantageous in condition monitoring as traveling on different road surfaces affects the wear of the vehicle in different ways. The benefits and drawbacks of the equipment used were assessed in order to establish which is the most efficient at road surface detection.

To estimate road surface a car was equipped with seven strategically placed accelerometers and data acquisition devices to gather data. The car was then driven upon asphalt and gravel roads of varying quality. Data was also gathered from the cars CAN-bus.

The acquired data was analysed using Peter D. Welch's power spectral density estimate to identify differences between the two surfaces. Magnitude squared coherence was used to determine the relation between the accelerometers.

While the study suggests that road surface detection by the means of measuring acceleration seems achievable. The results need to be verified with larger sets of data. The thesis concluded that not all accelerometers mounted were needed as many showed the same results. Measuring the acceleration of the vehicles suspension acceleration was deemed to be the most accurate way to estimate road surface.

Keywords: Road surface detection, accelerometer, Power spectral density, coherence

Acknowledgements

We have many people to thank in this section but mainly a big thank you to Matthijs Klomp och Fredrik Bruzelius for guiding us through out these months when the study was conducted.
Miguel Neto for assistance with the accelerometer setup.
Anders Wilson and crew for fitting the car with the accelerometers and helping with the setup of them.
Thank you for helping us along the way.

Nils Twedmark, Gothenburg, June 2021

Victor Carlberg Dahl, Gothenburg, June 2021

Contents

List of Figures **xi**

1 Introduction **1**
1.1 Background . . . 1
1.2 Aim . . . 2
1.3 Limitations . . . 2
1.4 Specification of issue under investigation . . . 3

2 Theory **5**
2.1 Welch's power spectral density estimate . . . 5
2.2 Magnitude-squared coherence . . . 5

3 Methods **7**
3.1 Tests . . . 7
3.2 Equipment . . . 8
3.3 Mounting the test equipment . . . 13
3.3.1 Accelerometers mounted on the shock absorbers . . . 13
3.3.2 Accelerometers mounted on the chassi . . . 15
3.3.3 Data acquisition devices . . . 17
3.4 Configuring the setup . . . 17

4 Data compilation and analysis **19**
4.1 Introduction . . . 19
4.2 Coherence . . . 19
4.2.1 Coherence of the single-axis accelerometers . . . 20
4.2.2 Coherence between the three-axis accelerometers . . . 22
4.2.3 Coherence of the vehicle suspension . . . 26
4.2.4 Coherence between the internal signals in the three-axis accelerometers . . . 27
4.3 The influence of velocity . . . 31
4.3.1 Asphalt . . . 31
4.3.2 Gravel . . . 36
4.4 Engine vibrations . . . 41
4.5 Comparing asphalt to gravel . . . 46
4.5.1 single-axis accelerometers . . . 46
4.5.2 Vehicle suspension acceleration . . . 49
4.5.3 Three-axis accelerometers . . . 53

5 Conclusion **65**
5.1 Estimating road surface 65
5.2 Presenting and interpreting data 65
5.3 What signals are useful at estimating road surface 66
5.3.1 Single-axis accelerometers 66
5.3.2 Three-axis accelerometers 66
5.3.3 Vehicle suspension acceleration 67
5.4 The most efficient signals for estimating road surface 68
5.5 Going forward 68

Bibliography **69**

List of Figures

3.1 Front view of the car . . . 8
3.2 Side view of the car . . . 8
3.3 Entran accelerometer . . . 9
3.4 DEWEsoft SIRIUS . . . 9
3.5 DYTRAN 3023A2 . . . 10
3.6 Piezo-electric amplifier . . . 10
3.7 DEWE-43A . . . 10
3.8 Vertical, Horizontal and Longitudinal axes along the car . . . 11
3.9 Breakout cable . . . 11
3.10 Logitech C310 . . . 12
3.11 GlobalSatBU-353S4 . . . 12
3.12 USB hub . . . 12
3.13 The two front three-axis accelerometers . . . 14
3.14 The two rear three-axis accelerometers . . . 14
3.15 Open hood of the car . . . 15
3.16 Trunk of the car . . . 16
3.17 Dewesoft data collecting hub . . . 17

4.1 Coherence between front left and right single-axis accelerometers . . . 20
4.2 Coherence between front left and rear single-axis accelerometers . . . 21
4.3 Coherence between front left and right three-axis accelerometers . . . 22
4.4 Coherence between rear left and right three-axis accelerometers . . . 23
4.5 Coherence between front and rear left three-axis accelerometers . . . 24
4.6 Coherence between front and rear right three-axis accelerometers . . . 25
4.7 Coherence of the vehicles suspension acceleration . . . 26
4.8 Coherence between front right axes . . . 27
4.9 Coherence between front left axes . . . 28
4.10 Coherence between rear right axes . . . 29
4.11 Coherence between rear left axes . . . 30
4.12 Suspension acceleration, 30 km/h in blue and 50 km/h in orange . . . 31
4.13 Left Front accelerometers . . . 32
4.14 Right Front accelerometers . . . 33
4.15 Left rear accelerometers . . . 34
4.16 Right rear accelerometers . . . 35
4.17 Vertical suspension acceleration . . . 36
4.18 Left front accelerometers . . . 37

4.19 Right front accelerometers 38
4.20 Left rear accelerometers 39
4.21 Right rear accelerometers 40
4.22 Vertical suspension acceleration 41
4.23 Left Front accelerometers 42
4.24 Right Front accelerometers 43
4.25 Left rear accelerometers 44
4.26 Right rear accelerometers 45
4.27 Left front single-axis accelerometer 46
4.28 Right front single-axis accelerometer 47
4.29 Rear single-axis accelerometer 48
4.30 Right front suspension 49
4.31 Left front suspension 50
4.32 Right rear suspension 51
4.33 Left rear suspension 52
4.34 Right front horizontal axes 53
4.35 Right front vertical axes 54
4.36 Right front longitudinal axes 55
4.37 Left front horizontal axes 56
4.38 Left front vertical axes 57
4.39 Left front longitudinal axes 58
4.40 Left rear horizontal axes 59
4.41 Left rear vertical axes 60
4.42 Left rear longitudinal axes 61
4.43 Right rear horizontal axes 62
4.44 Right rear vertical axes 63
4.45 Right rear longitudinal axes 64

1
Introduction

This chapter will go through the background, aim, limitation and specific issues of this bachelor thesis.

1.1 Background

Every car that is being used needs to be kept under maintenance. If something breaks or needs to be replaced the car has to go in to the garage. This costs both time and money. Volvo wants to make this process shorter and cheaper to make their cars more driver friendly. One way of reducing the time and money spent on repairing a car that breaks down is by not having it break down in the first place. This can be done by having predictive maintenance and a major part of predictive maintenance is condition monitoring.

Condition monitoring is a method for overseeing the wear of a system, machine, wear part etcetera, by continuous or periodical monitoring. This can be done by identifying certain key aspects that are crucial for the longevity of the system. In some systems an ocular inspection once in a while can be deemed enough while others are more complex such as monitoring the wear of shock absorbers of a car.

Another part of condition monitoring is being able to classify the driving style of a driver. One example of that is what kind of road surface the car is being driven on. This thesis will go in more depth how one can recognize the road surface and try to determine the best way of doing this.
Road surface estimation is not a new field of research so as to determine how to efficiently deduce something not explored before, a literature study was performed.

From the study it was concluded that there are many ways of approaching this topic and the information on the road surface estimation can be used in many different ways. For example there are several studies which use visual based detection. For example “Vision based road surface detection for automotive systems” which identifies a use in improving Antilock Braking System(ABS) “Vision based road surface detection for automotive systems” [1], “Advance information about the road surface a vehicle is going to encounter can improve the performance of automotive systems. For e.g. the initial slip cycles caused by the Antilock Braking Systems (ABS) could be avoided, if it is already known that the vehicle is on a surface having a low coefficient of friction (μ).”

There are studies which use Light Detection and Ranging(LIDAR). One paper [2] uses LIDAR to improve maintenance of roads "ROAD SURFACE DETECTION FROM MOBILE LIDAR DATA".

Also several studies which use the accelerometers in the smartphone to estimate road surface, for instance [3] "A Mobile Application for Road Surface Quality Control: UNIquALroad".

From the papers presented above and several others the following two main statements could be concluded. Detecting road surface can be done in several different ways depending on the purpose of the data collected. Detecting road surface can be done but road surface classification(fitting the data into a model) is a remaining problem in many of the studies included in the literature study.

With the scope being condition monitoring as a part of predictive maintenance it was derived that using accelerometers to monitor the forces acting on the car would fit the purpose well. As the raw data from the accelerometers can be used in further studies of how much force certain wear parts can take before failing.

1.2 Aim

The scope of this thesis is road surface estimation as a part of condition monitoring. Today little is known about which surface a car is being operated upon once in the hands of a consumer. This thesis will explore what signals can be useful and how effective they are at identifying road surfaces.

1.3 Limitations

With road surface estimation being a broad topic with a lot of possibilities and variables. There is a need to set some limitations in order to be able to complete the work within the given time frame.

One limitation is that it is only one car being tested during the entirety of this report. This means that the data collected will only come from that same car consequently, phenomena that is discovered here might be unique to this individual vehicle. Going further in that direction, there will only be one setup of how the test equipment is mounted.

Another limitation is that not all types of road surfaces will be available to collect data from. The data collected in this report comes from road surfaces on tracks from Volvo's Proving Ground in Hällered and roads in and around Gothenburg.

This report will mainly focus on the possibility to reliably estimate what type of road a car is being operated upon. The data collected and conclusion drawn from this

thesis can be useful in exploring predictive maintenance and condition monitoring further, but will not be done here.

1.4 Specification of issue under investigation

- Is it possible to estimate what road surface the vehicle is traveling upon?
- Which signals are the most efficient at estimating road surface?
- What is the best way to interpret the data collected?
- What is the best way to present the (if identified)patterns?

2
Theory

To analyse the data that were recorded by the Dewesoft equipment in a effective way two methods were mainly used. This chapter will explain the theory behind these methods.

2.1 Welch's power spectral density estimate

Welch's power spectral density estimate [4] is a method for spectral density estimation named after Peter D. Welch, Ph.D which presented it in 1967 in IEEE Transactions on Audio and Electroacoustics. The method is often used in vibration analysis to approximate the power of a signal at various frequencies. Another common way of doing this is the FFT(Fast fourier transform) however Welch's method reduces the noise in the estimation, which is why it was the chosen tool for the analysis.

2.2 Magnitude-squared coherence

Magnitude-squared coherence [5] is a way of evaluating the coherence between two sets of data. The coherence function estimates, for each frequency, the ratio of the signal power to total power. Magnitude-squared coherence indicates if a given input and output are linearly related. The coherence ranges from 0 to 1 where 1 indicates perfectly linear relationship and 0 indicates no correlation.

$$MSC(f) = \frac{|P_{xy}(f)|^2}{P_{xx}(f).P_{yy}(f)} \tag{2.1}$$

3
Methods

To collect data, a car was fitted with four accelerometers mounted on the shock absorbers and three mounted on the chassi. Data was also collected from the CAN-bus. These accelerometers were connected to a synchronous data collection device.

3.1 Tests

In accordance with the aim of the thesis the tests tried to simulate the driving habits of the average driver and see if it is possible to deduce anything valuable. It is hard to determine what the average driver profile is and it's quite an ambiguous statement.
To better convey the meaning of this statement:

- The tests were performed on public roads with traffic present.
- The driving complied with Swedish driving regulations.
- The nature of the driving was economical and with moderate to low accelerations.

The tests were carried out at different speeds ranging from crawling speeds up to 110km/h on asphalt. On gravel the top velocity was limited to 50km/h as no roads found allowed for higher speeds. Once the data had been acquired it was used to draw conclusions and identify patterns.

Other than driving and collecting data two specific tests were conducted.

- To test how different velocities affected data acquisition tests when conducted on the same piece of road driving at different speeds.
- To see how the vibrations of the engine affected the data acquired a test was performed when standing still and revving the engine in a controlled fashion.

3.2 Equipment

The car that the tests were performed with is a Volvo XC60 T6 AWD Geartronic, 2018. In total seven accelerometers was fitted on the car, on top of production vehicle fitted sensors that was acquired from the CAN-bus. In figure 3.1 and 3.2 is the car that was used for these tests.

Figure 3.1: Front view of the car

Figure 3.2: Side view of the car

The accelerometers used for the chassi were three (Entran EGCS-SO24D-50) accelerometers as seen in figure 3.3. Accelerometers on the chassi will measure force only in the vertical direction and the magnitude of the signal is 100 mV/g. These accelerometers are used to see if the acceleration of the sprung mass of the car could be useful in estimating what type of road surface is being driven on and if so what the correlation is to the unfiltered vibrations measured by the remaining four.

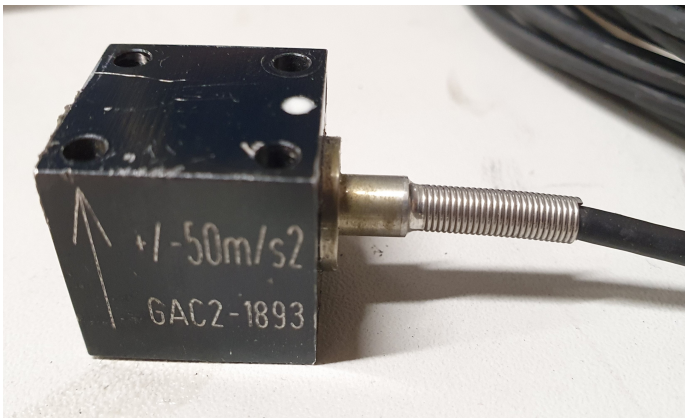

Figure 3.3: Entran accelerometer

To connect the three accelerometers on the chassi a DEWEsoft SIRIUS-STG-8 shown in figure 3.4 was used in order to synchronize and record the data collected.

Figure 3.4: DEWEsoft SIRIUS

Four (DYTRAN 3023A2) accelerometers were connected with piezo-electric amplifiers to two different dewesoft dewe-43a seen in shown in figure 3.5-3.7. These four accelerometers were placed on the shock absorbers in order to record the unsprung vibrations caused by the road surface. The accelerometers on each of the shock absorbers would measure force in three ways along the three axes Vertical, Horizontal and Longitudinal. The signal produced by these accelerometers was in the magnitude 10 mV/g.

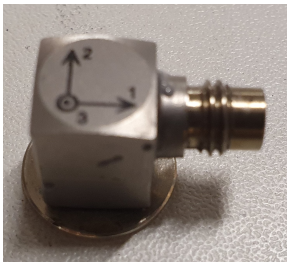

Figure 3.5: DYTRAN 3023A2

Figure 3.6: Piezo-electric amplifier

Figure 3.7: DEWE-43A

The three axis accelerometers were positioned so that the axes were lined up as the following figure 3.8.

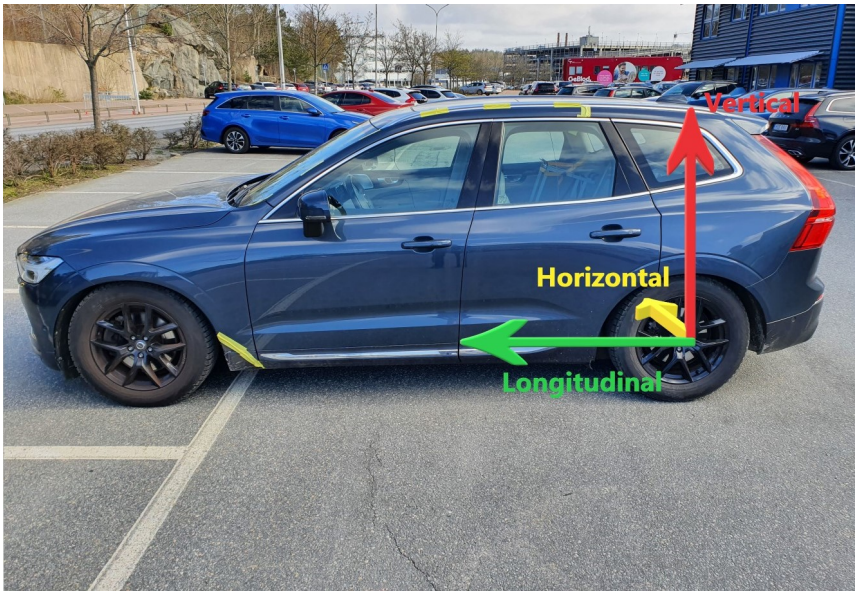

Figure 3.8: Vertical, Horizontal and Longitudinal axes along the car

The two dewe-43a are connected with synchronization cables to the SIRIUS in order to have time synchronization in all the data collection. A breakout cable from the car's chassi CAN-bus was also connected to the SIRIUS-8 as shown in figure 3.9 to get information about suspension position and other useful information. All of the three devices powered via the car's battery through the cigarette lighter socket and connected to a computer used to record and store the data.

Figure 3.9: Breakout cable

In order to be able to go back in the data and check what type of road the car was being driven on for reference, it was fitted with a webcam (Logitech C310) seen in figure 3.10 and a GPS (GlobalSatBU-353S4) shown in figure 3.11.

Figure 3.10: Logitech C310

Figure 3.11: GlobalSatBU-353S4

In order to connect the SIRIUS, the two dewe-43a, the webcamera and the GPS to the computer a USB hub shown in figure 3.12 was used.

Figure 3.12: USB hub

3.3 Mounting the test equipment

This section will go through and show how all the equipment was mounted on the car.

3.3.1 Accelerometers mounted on the shock absorbers

Figure 3.13 and 3.14 shows where the three-axis accelerometers were mounted on the spindles of the car. These accelerometers were placed so that they would get the unfiltered forces from the road surface.

Figure 3.13: The two front three-axis accelerometers

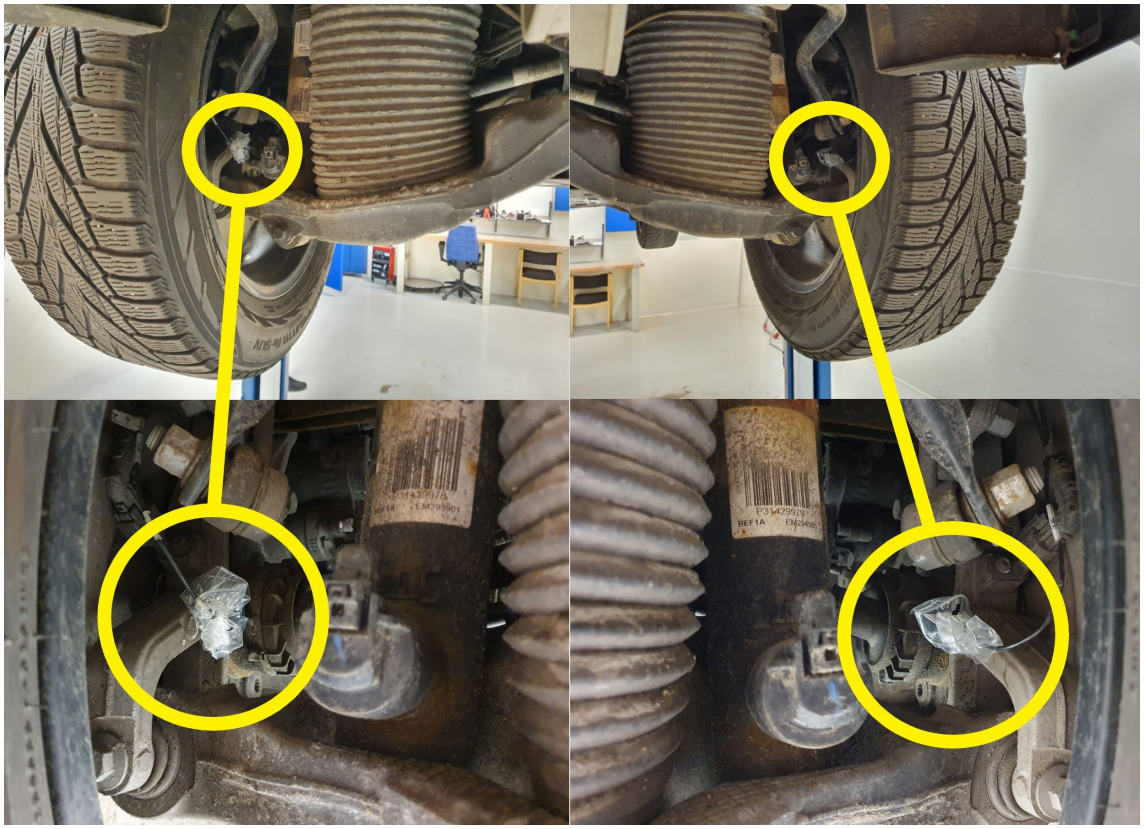

Figure 3.14: The two rear three-axis accelerometers

3.3.2 Accelerometers mounted on the chassi

Figure 3.15 shows how two of the three single-axis accelerometers are placed on the chassi on the spring housing.

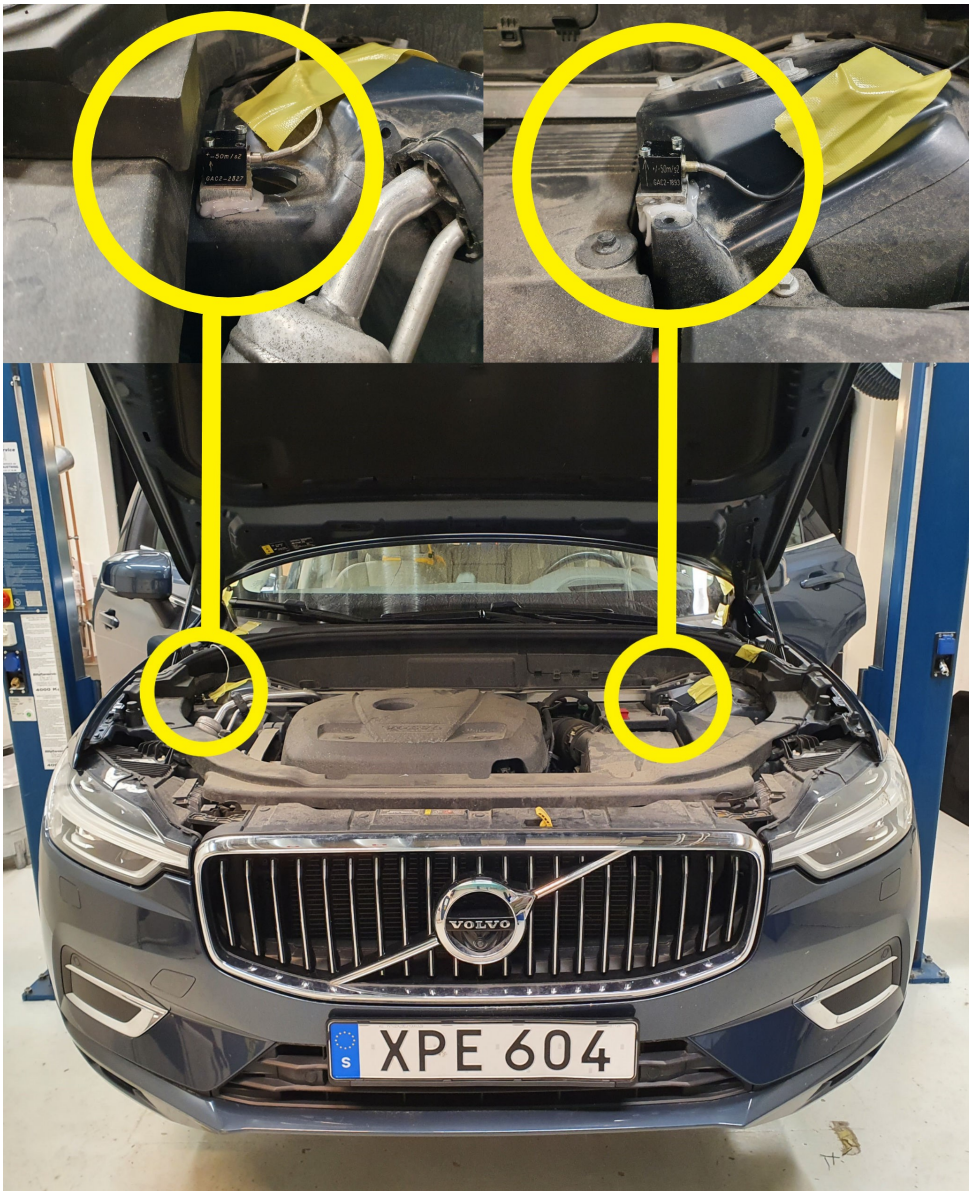

Figure 3.15: Open hood of the car

The last single-axis accelerometer was placed in the trunk of the car as seen in figure 3.16.

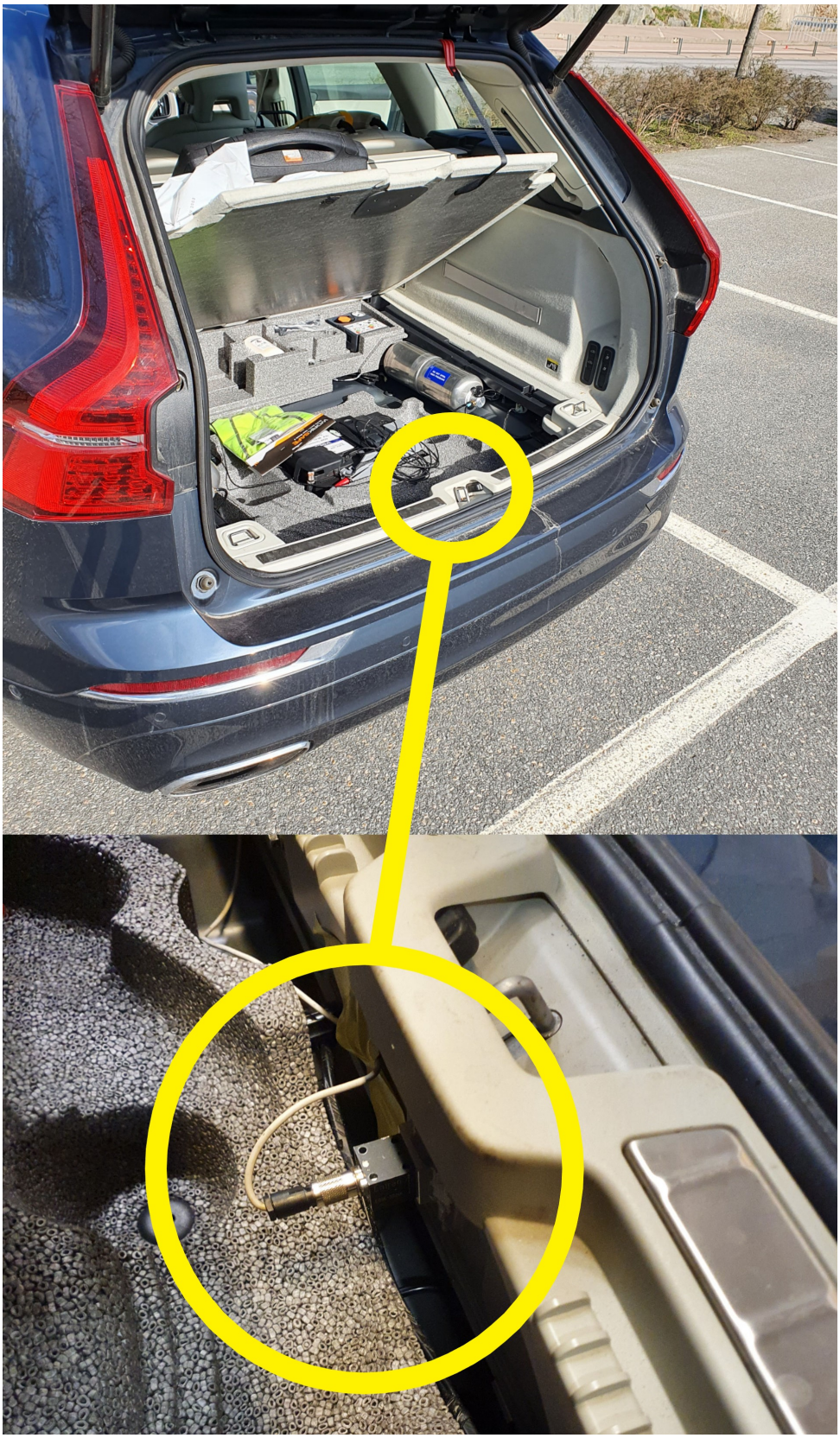

Figure 3.16: Trunk of the car

3.3.3 Data acquisition devices

When all the accelerometers were mounted and their cabling were pulled through the doors and trunk to the back seat of the car where they were connected to their data acquisition devices according to figure 3.17. The breakout cable from the chassi CAN-bus was pulled from below the steering wheel to the Sirius device. The devices themselves were mounted in an aluminum rack, to prevent them from moving during test drives. The rack was then fastened in the isofix mounts.

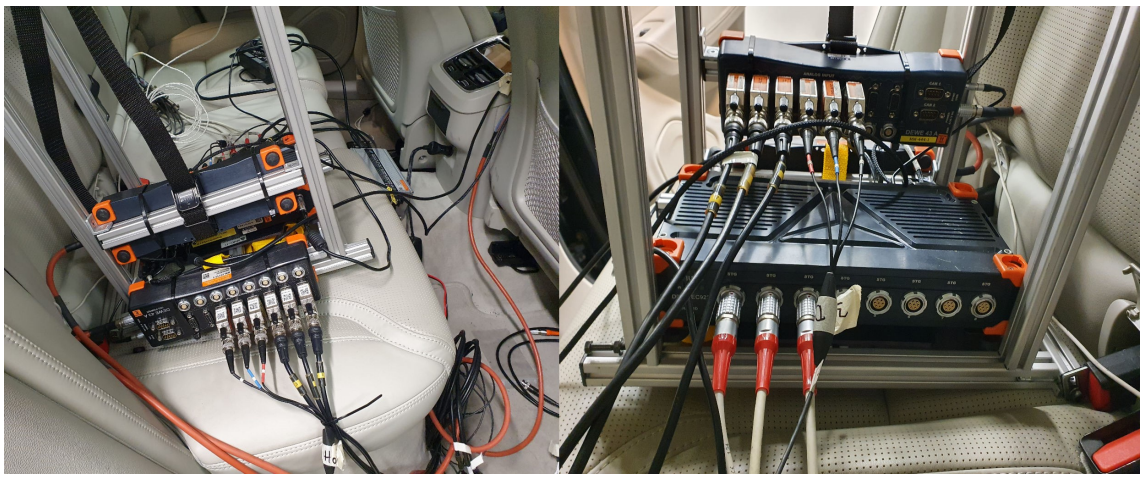

Figure 3.17: Dewesoft data collecting hub

When all the accelerometers had been connected to the dewe-43a s and the sirius they were then plugged in together with the chassiCAN to a USB-hub together with the web camera and GPS. The USB-hub was then connected to the computer.

The software used to store data was DEWEsofts own Dewesoft X3 SP12 73.12.20.0603. The software allows the selection of which channels of information are being used.

3.4 Configuring the setup

The accelerometers needed to be set up before the testing started so that they would give off correct measuments. The accelerometers were already calibrated when recived. The accelerometers were setup in DEWEsoft according to the data from the calibration certificates.

4

Data compilation and analysis

This chapter will go through the data collected and analyze it in order to be able to draw conclusions from it.

4.1 Introduction

In order to analyze the data acquired it was exported from Dewesoft X3 as '.mat' files which allowed importing it as a struct of arrays into Matlab. The data was then processed with the function pwelch in order to examine the power spectral density of the data with the reduced noise that pwelch offers in comparison to the fourier transform. When examining the relationships between signals the mscohere function was used. From these two functions plots were produced with the aim of analysis and comparison.

4.2 Coherence

Since the car has been fitted with many accelerometers it was decided that examining the coherence of the signals was the first measure. A high measure of coherence between the accelerometers would indicate that they show similar results. If accelerometers show the same data they can be excluded from certain parts of the analysis. The coherence was tested on a large set of data consisting of both asphalt and gravel driving.

The nature of vibration analysis makes these graphs hard to interpret as most signals were sampled at 1 kHz. There are a lot of 'jumps' from very coherent to non coherent. A mean of the total coherence of the signals was calculated and added as a line in some of the plots to portray the average overall coherence of the two signals being compared. While analysing certain domains where the signals can be especially divergent or consistent is important, a mean of the coherence can be useful as well.

4.2.1 Coherence of the single-axis accelerometers

As described in the method the car was fitted with three single-axis accelerometers. The coherence of the signals were analysed in this section.

When testing the coherence between the two single-axis accelerometers mounted on the left and right spring tower the following plot 4.1 was produced.

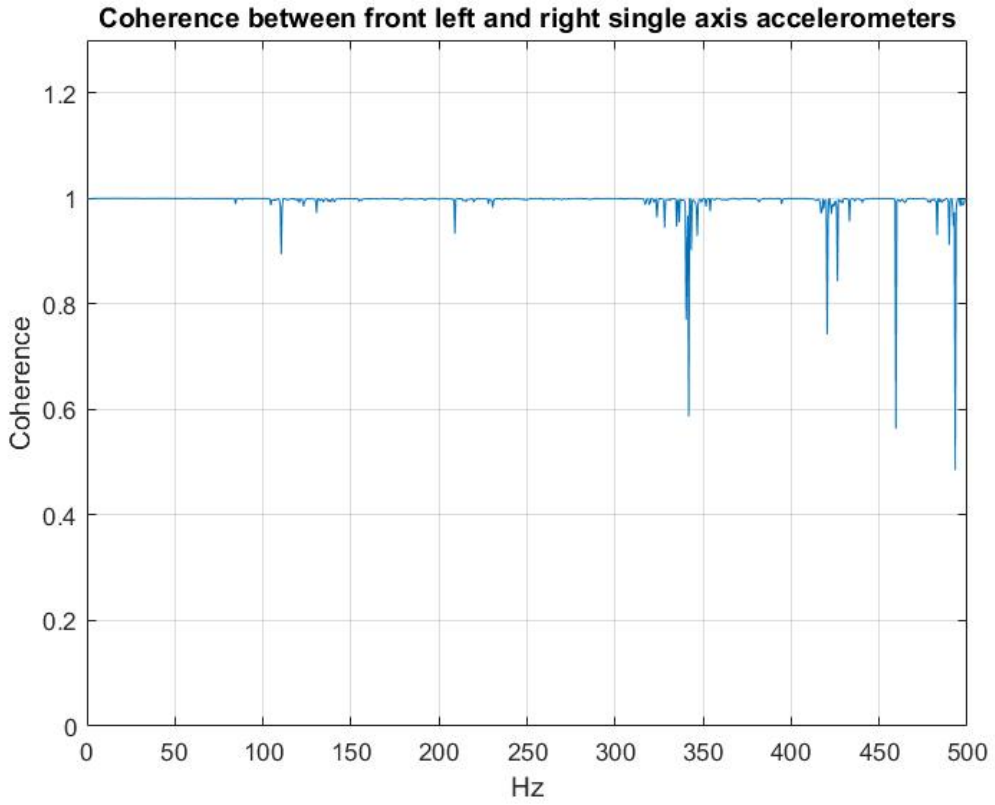

Figure 4.1: Coherence between front left and right single-axis accelerometers

The measure of coherence that can be seen in the plot is very close to one.

When investigating the coherence between the front left and rear accelerometer the following plot was produced in figure 4.2.

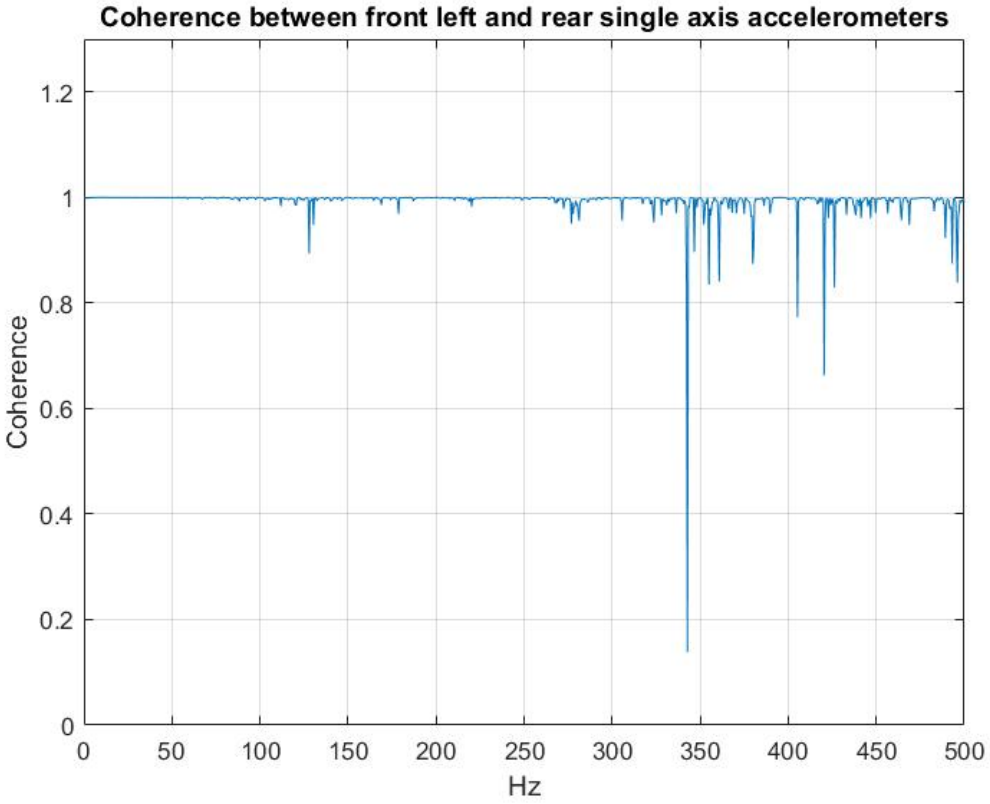

Figure 4.2: Coherence between front left and rear single-axis accelerometers

The coherency between the front left and rear single-axis accelerometers is high; close to one.

These two graphs suggest that the three single-axis accelerometers mounted on the chassi of the car produce very similar signals. It can be concluded that two out of three single-axis accelerometers are redundant in this thesis work and that the placement on the chassi is irrelevant.

4.2.2 Coherence between the three-axis accelerometers

In this segment the coherence between the three different axes of the accelerometers mounted on each spindle of the vehicle was inspected.

First the relationship between front left and right accelerometer was looked into and the following cluster of plots was produced in figure 4.3.

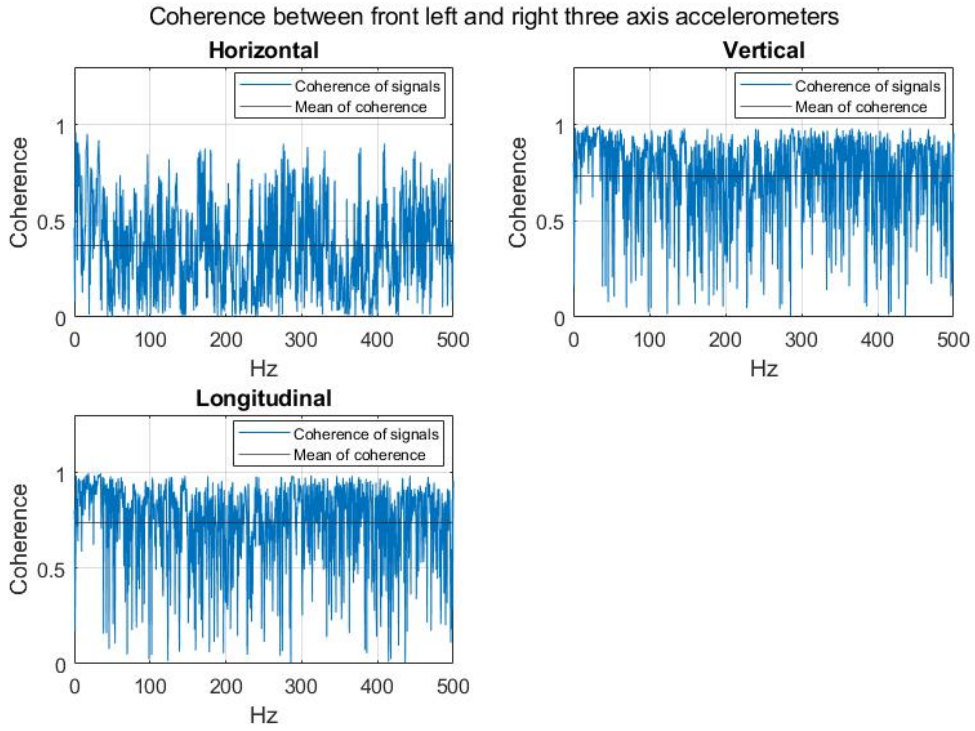

Figure 4.3: Coherence between front left and right three-axis accelerometers

Each of the graphs show the measure of coherence between one of the axes of the accelerometer on the left and the right. The coherence between the two horizontal axes is overall low, with a mean of 0.4. Both the vertical and longitudinal axes show high coherence between the right and left accelerometers, the mean being 0.75. Although the mean is high there are some regions of frequency that the coherence is poor.

In figure 4.4 the following cluster of plots shows the coherence between the rear left and right accelerometers.

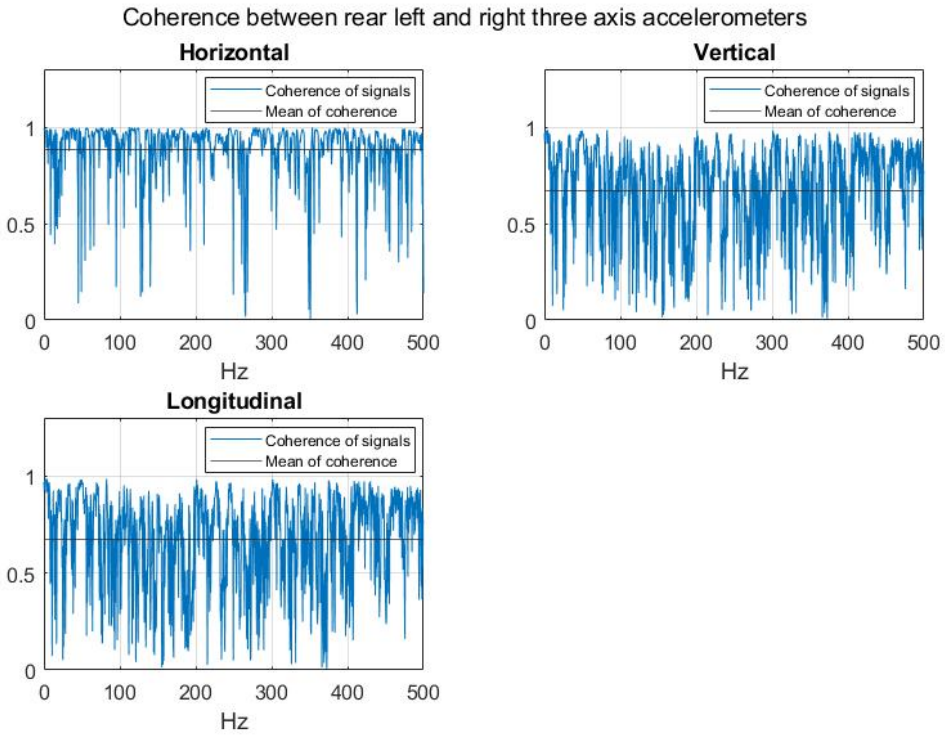

Figure 4.4: Coherence between rear left and right three-axis accelerometers

Between the rear horizontal axes the coherence is very high across the board with some plunges, the mean is 0.9. As in the previous graph the mean of the coherence signal is very similar for the vertical and longitudinal axes, albeit a little lower at 0.7 compared to 0.75 for the front.

The subsequent cluster of plots in figure 4.5 shows the coherence between the front and rear left accelerometers.

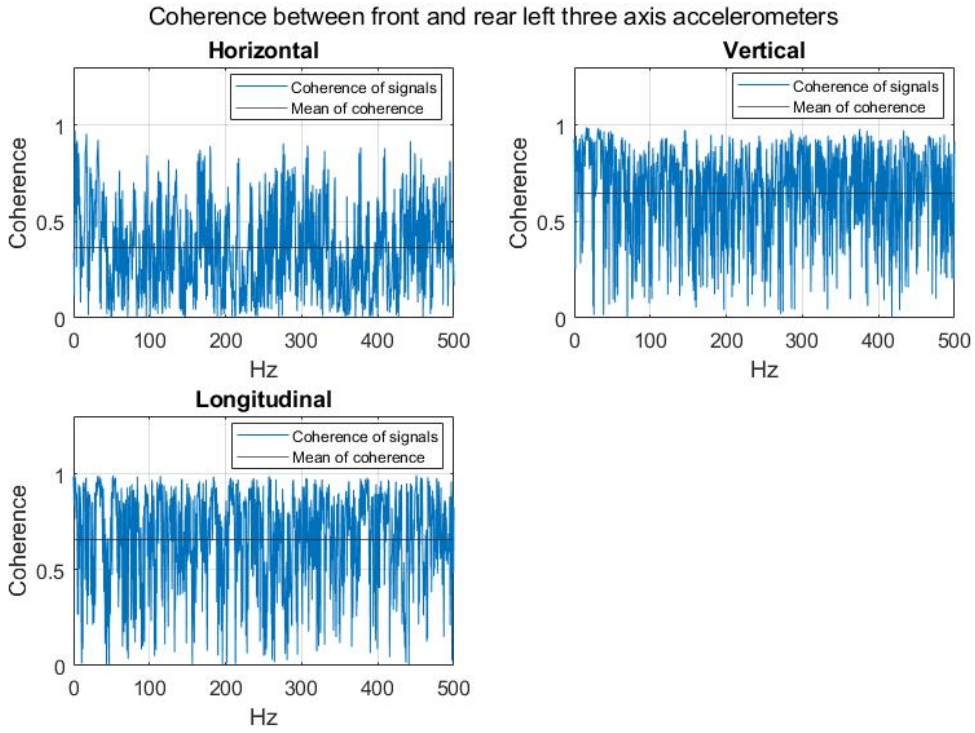

Figure 4.5: Coherence between front and rear left three-axis accelerometers

Coherence between front and rear left three-axis accelerometers. It can be seen that the coherence of the horizontal axes is low, with the mean being 0,4. While the vertical and longitudinal axes have a higher measure of coherence with the average of a little less than 0,7. These plots show great similarities to the plots of the comparison between the front left and right accelerometers.

The next cluster of plots in figure 4.6 portrays the coherence between the front and rear right accelerometers.

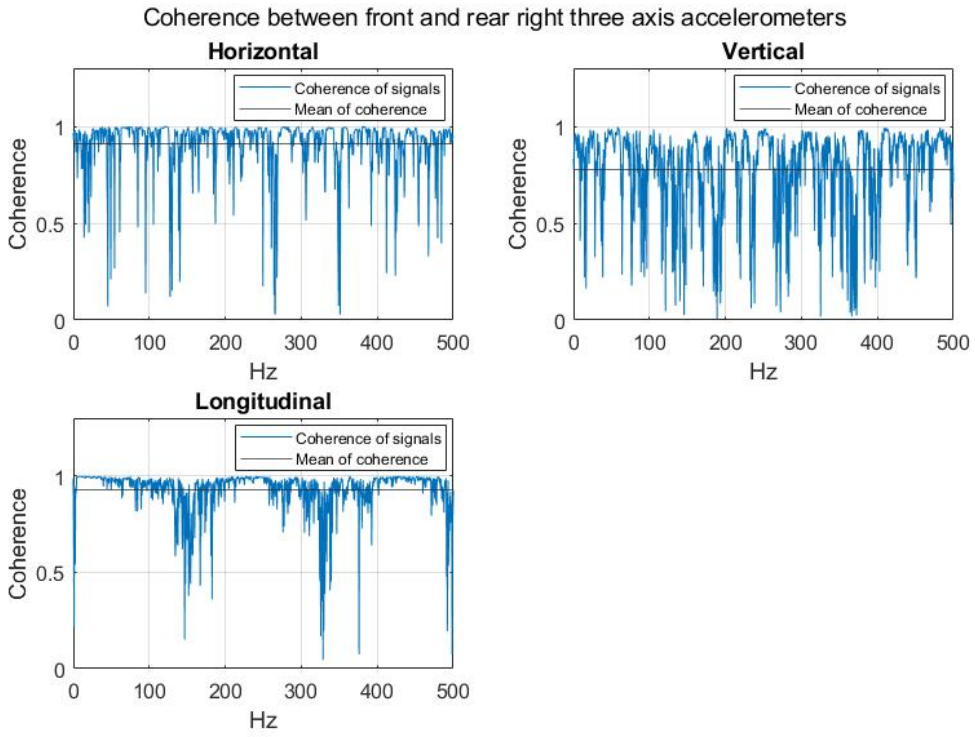

Figure 4.6: Coherence between front and rear right three-axis accelerometers

All three plots in this figure show a great measure of coherence, especially for the horizontal and longitudinal axes, both averaging above 0.9. The vertical axes show a little less coherence with a mean a little shy of 0.8.

The result of this coherency comparison is not as clear cut as for the single-axis accelerometers. While the mean of coherency is a good measure of the overall relation between the signals there are regions with low relation to each other. These regions might contain important data and therefore no accelerometers analysed in this segment can be excluded from the analysis on the merit of coherence alone. However, this result in combination with further analysis can prove useful.

4.2.3 Coherence of the vehicle suspension

This portion of the analysis will investigate the coherence of the suspension acceleration. The channel on the CAN-bus in figure 4.7 containing the vehicle suspension acceleration has an update rate of 67 Hz as compared to the mounted accelerometers 1000 Hz.

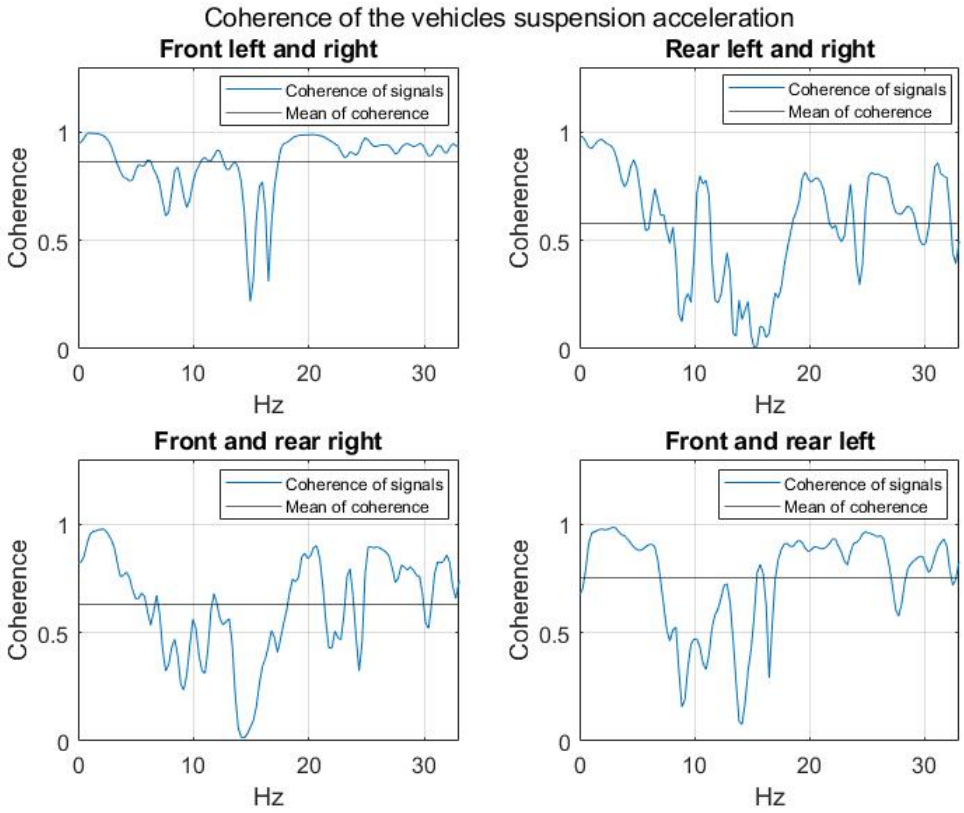

Figure 4.7: Coherence of the vehicles suspension acceleration

The front left and right suspension overall has high coherence, with the only two significant plunges at 15 and 17 Hz. The mean coherence being 0.83.
The rear left and right suspension shows a lower overall coherence, especially in the regions 8-9 and 12 to 17 Hz. With a mean coherence of 0.59.
The front and rear right suspension has a little higher mean coherence of 0.62 with and is particularly incoherent around 15 Hz.
For the front and rear left suspension the mean coherence is quite high at 0.78 and plummets in coherence between 8 and 17 Hz.

Overall the coherence between the four different suspension acceleration is quite high, but not high enough to exclude any of these signals on this result solely.

4.2.4 Coherence between the internal signals in the three-axis accelerometers

In the last part of this coherence investigation the coherence between the internal axes of the three-axis accelerometers were assessed.

Below four clusters of plots are presented with three subplots each. Looking at the subplots within a cluster the three axes of the accelerometers are compared to each other, Vertical vs Horizontal, Vertical vs Longitudinal and Horizontal vs Longitudinal.

Beneath in figure 4.8 is the coherence comparison for the front right three-axis accelerometer.

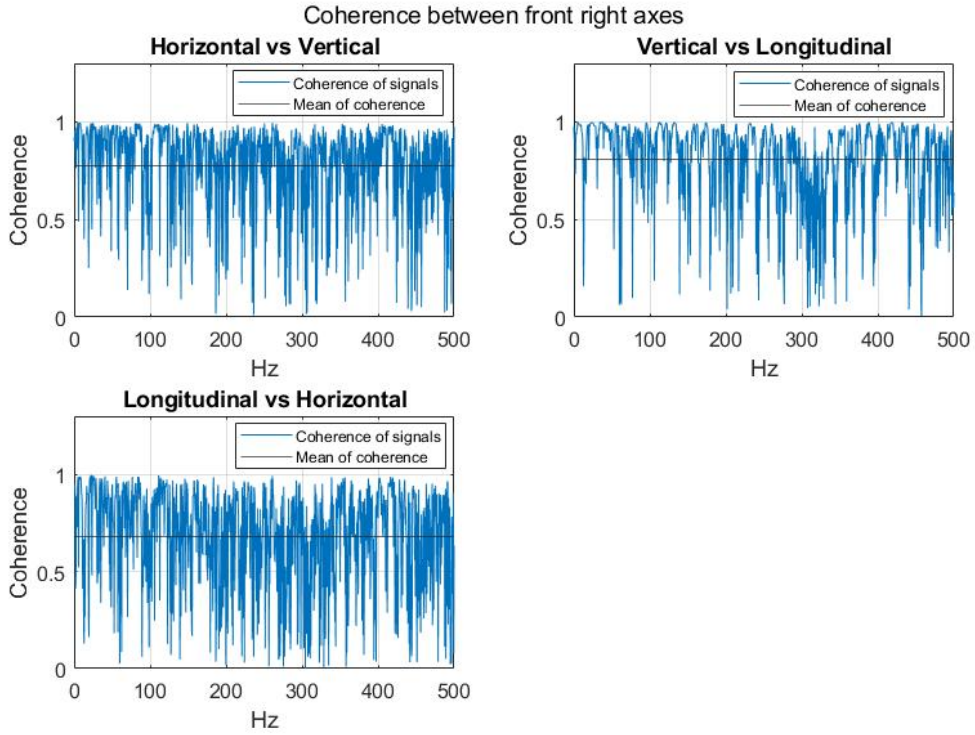

Figure 4.8: Coherence between front right axes

When examining the plots for the front right three-axis accelerometer both the horizontal and longitudinal axes seem to correlate highly with the vertical axis, with the average coherence being 0.8 for the vertical and longitudinal and close to 0.8 for the horizontal and vertical. The coherence is especially high around 400Hz and worse around 300 Hz. Longitudinal and horizontal axes coheres marginally worse with an average of 0.7 with a peak coherence at 400Hz.

The following cluster of plots in figure 4.9 shows the coherence between the three axes in the front left accelerometer.

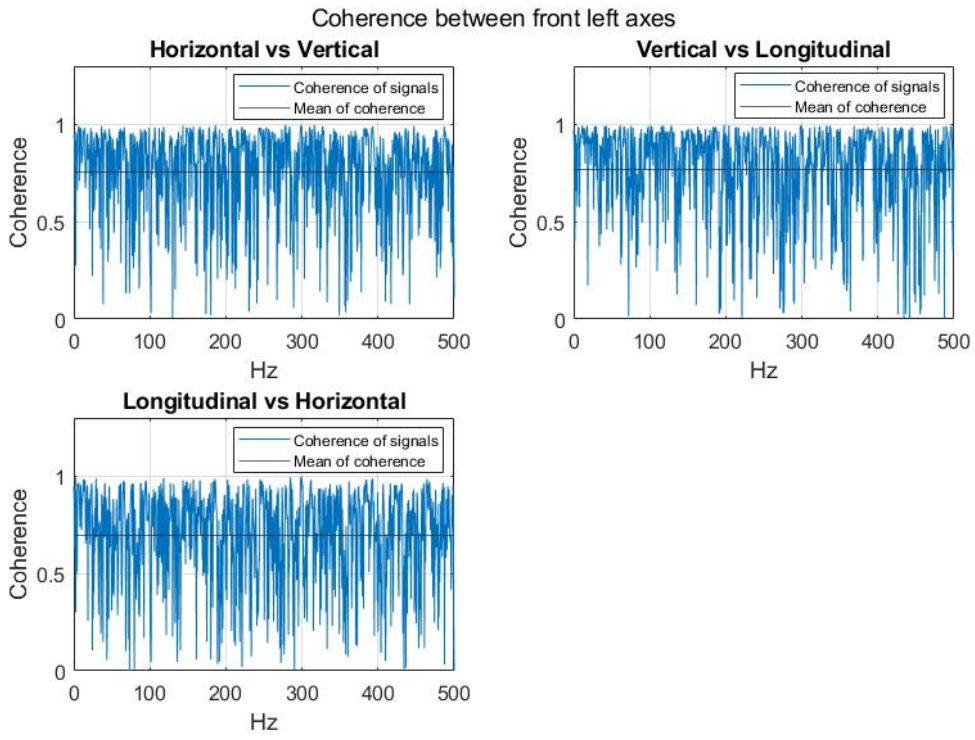

Figure 4.9: Coherence between front left axes

The front left accelerometers axes show the same results as the front right axes, with a higher coherence between the vertical axis to the horizontal and longitudinal with a mean coherence of approximately 0.8. The coherence between the longitudinal and horizontal is lower at 0.7.

The rear right axes are compared in the subsequent cluster of plots in figure 4.10.

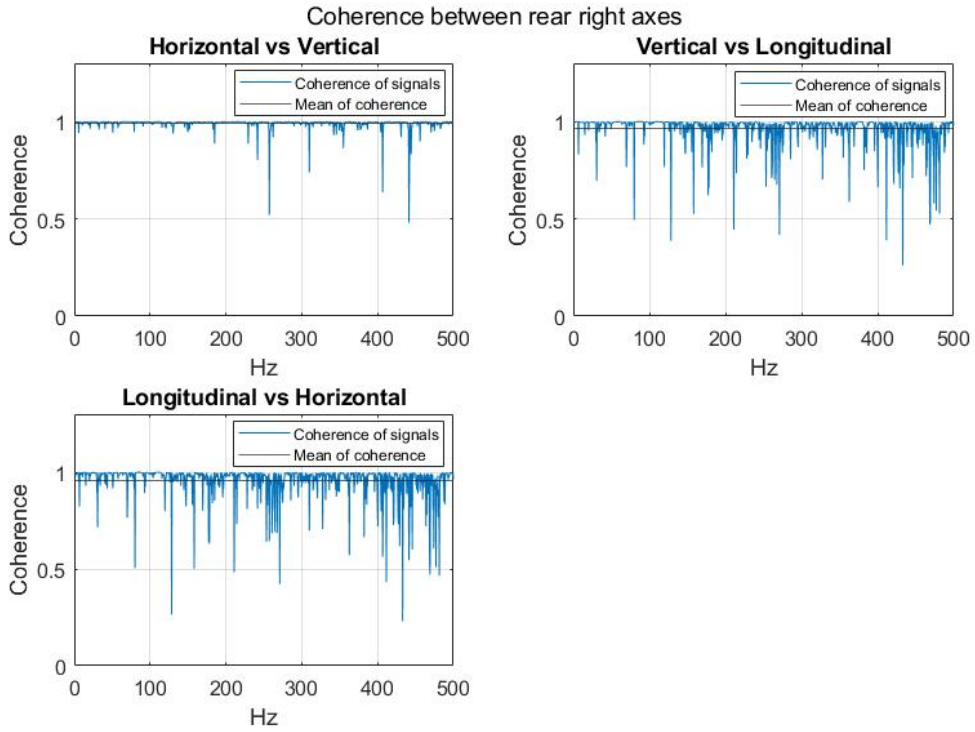

Figure 4.10: Coherence between rear right axes

The rear right accelerometer axes show very high coherence with an average of almost one.

Lastly, the rear left accelerometer in figure 4.11.

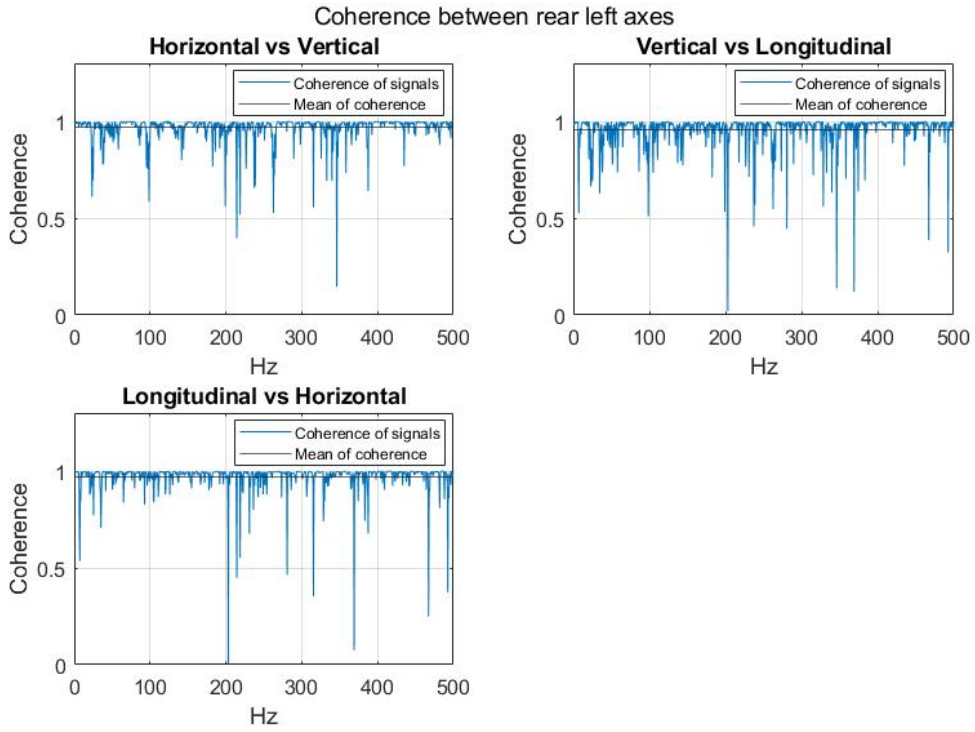

Figure 4.11: Coherence between rear left axes

In a very similar manner to the rear right axes the left axes show the same coherence of nearly one.

Across the board there is very high coherence between the internal axes of the three-axis accelerometers, especially for the rear accelerometers. This suggests that a single-axis accelerometer provides very similar data when mounted on the rear spindles as the three-axis accelerometer. The front accelerometers portray a different picture. While the coherence overall is high further investigation will be needed in order to assess which of the axes produces the best signal for road surface monitoring.

4.3 The influence of velocity

In order to see how velocity affects the accelerometers two sets of data were analysed. One set of data acquired while driving 30 km/h on asphalt and then driving the same stretch of road at a pace of 50km/h. Another set of data was collected using the same method but on gravel instead.

4.3.1 Asphalt

Five clusters of plots will be presented here, one for the suspension acceleration acquired from the CAN-bus and four clusters for each respective three-axis accelerometer mounted on the spindle.

The following four plots in figure 4.12 compare the power content of the two different velocities in the suspension.

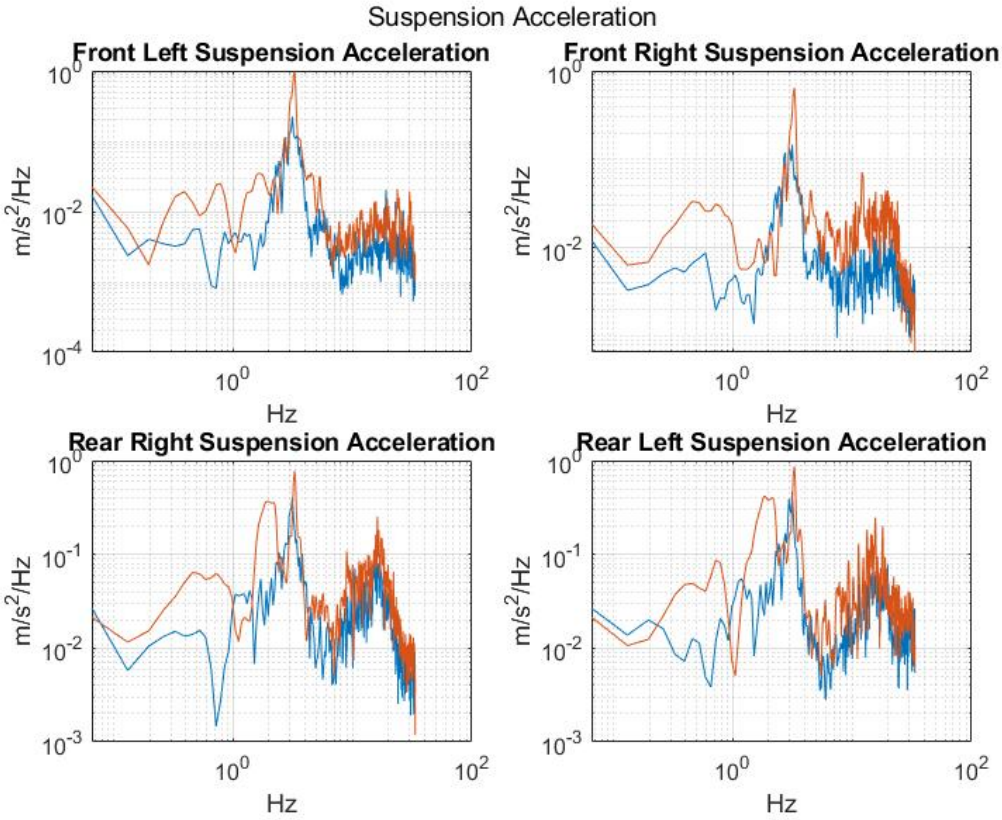

Figure 4.12: Suspension acceleration, 30 km/h in blue and 50 km/h in orange

In general the two different paces produce similar signals. The faster pace produces a signal with a moderately higher power content. The signal of the front suspenders shows a greater difference in amplitude between the two velocities in the region below 25Hz, compared to the rear suspenders. At frequencies above 25 Hz the two signals start to converge into each other.

The next cluster of plots in figure 4.13 represent the two accelerometers mounted on the left spindle and spring tower.

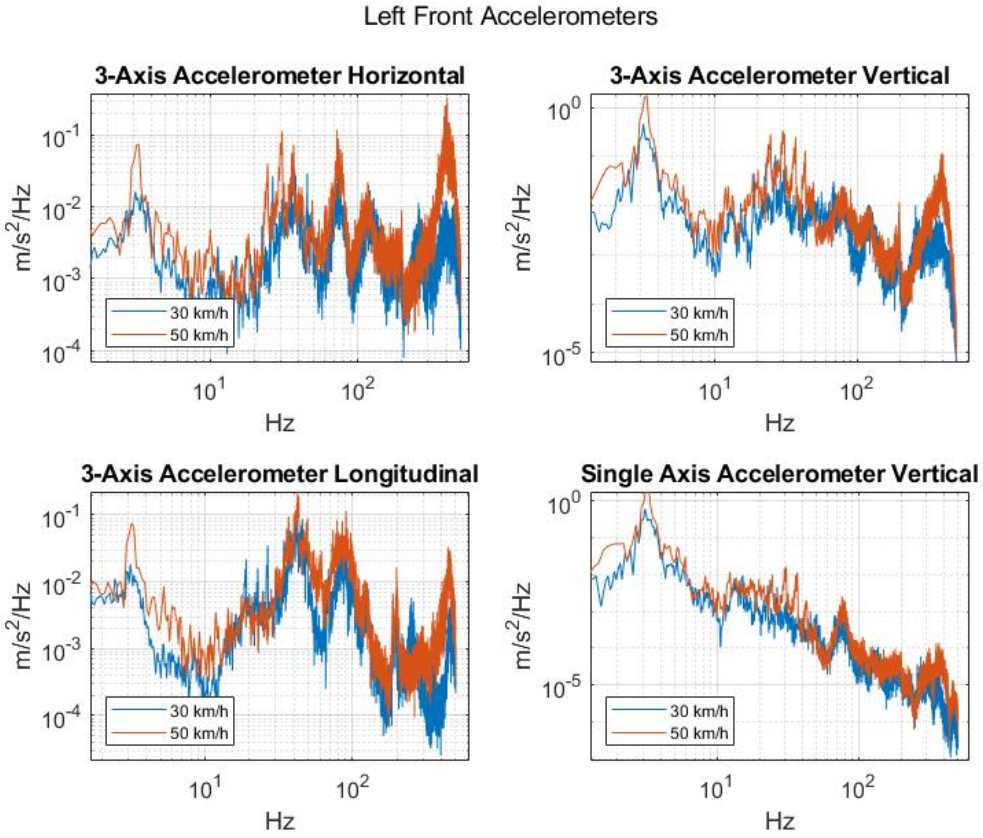

Figure 4.13: Left Front accelerometers

For the front left accelerometers there is less of a difference in power as compared to the suspension of the vehicle. However, in the domain between 15-40 and 300-490 Hz the three-axis accelerometers vertical and horizontal directions, there is a difference in amplitude. The single-axis accelerometer portrays some spikes in the same domains as the three-axis accelerometers but less distinct.

The subsequent four plots show the signals for the accelerometers mounted on the front right spindle and feather tower.

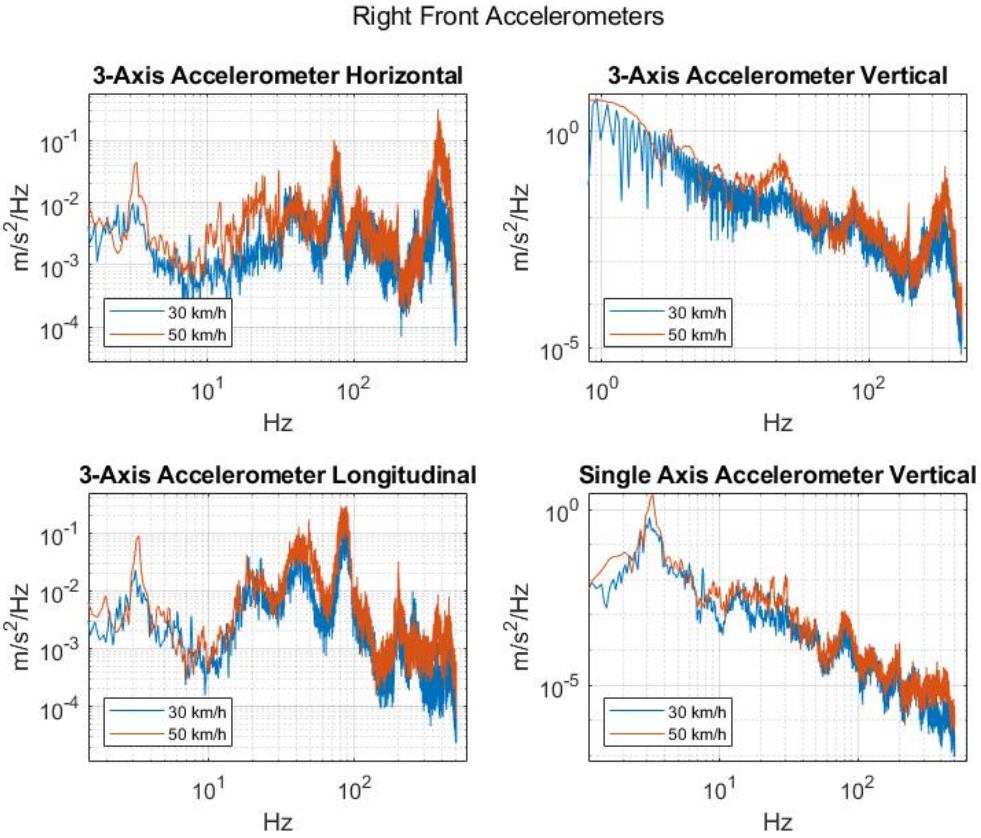

Figure 4.14: Right Front accelerometers

Looking at the right front accelerometers the three-axis horizontal and longitudinal as well as the single-axis accelerometer is very similar to each respective accelerometer shown in the previous figure. The vertical direction of the three-axis accelerometer, the slower pace signal shows much more acceleration at lower frequencies than any set of data previously analysed. The higher speed signal portrays high resemblance to the high speed signal of the respective accelerometer direction mounted on the front left spindle.

The signals for the left rear spindle and trunk accelerometer are presented in the following cluster of plots in figure 4.15.

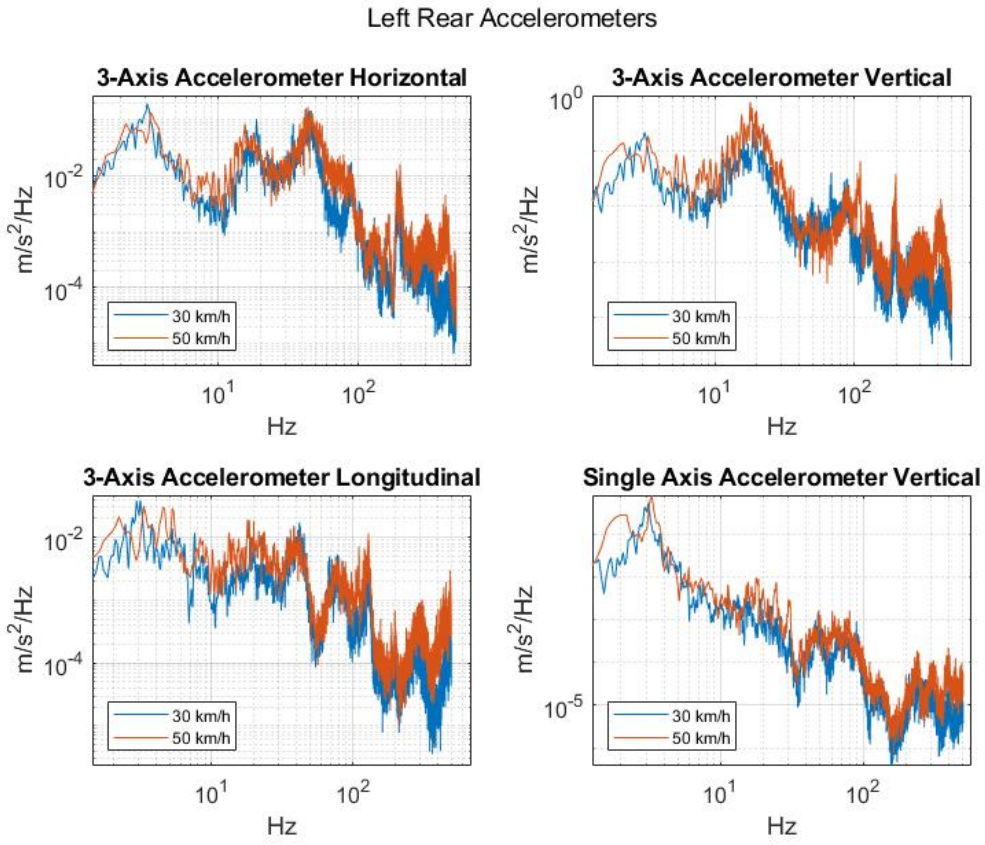

Figure 4.15: Left rear accelerometers

The left rear accelerometers overall portrays the same trends as identified in the front left accelerometers, with the key exception of a significant drop in power content of the signals in the region above 400 Hz. The vertical axis of the spindle mounted accelerometer shows a difference in amplitude of the signals of the two paces in the domain between 1-40Hz.

The last cluster of plots in figure 4.16 show the signals of the right rear spindle accelerometer and the trunk accelerometer.

Figure 4.16: Right rear accelerometers

The rear right accelerometers show very similar signals as to the left rear accelerometers.

4.3.2 Gravel

In the same way as the comparison on asphalt five clusters of plots will be presented here, one for the suspension acceleration acquired from the CAN-bus and four clusters for each respective corner of the car.

The power content of the vehicle's suspension acceleration is presented below in figure 4.17.

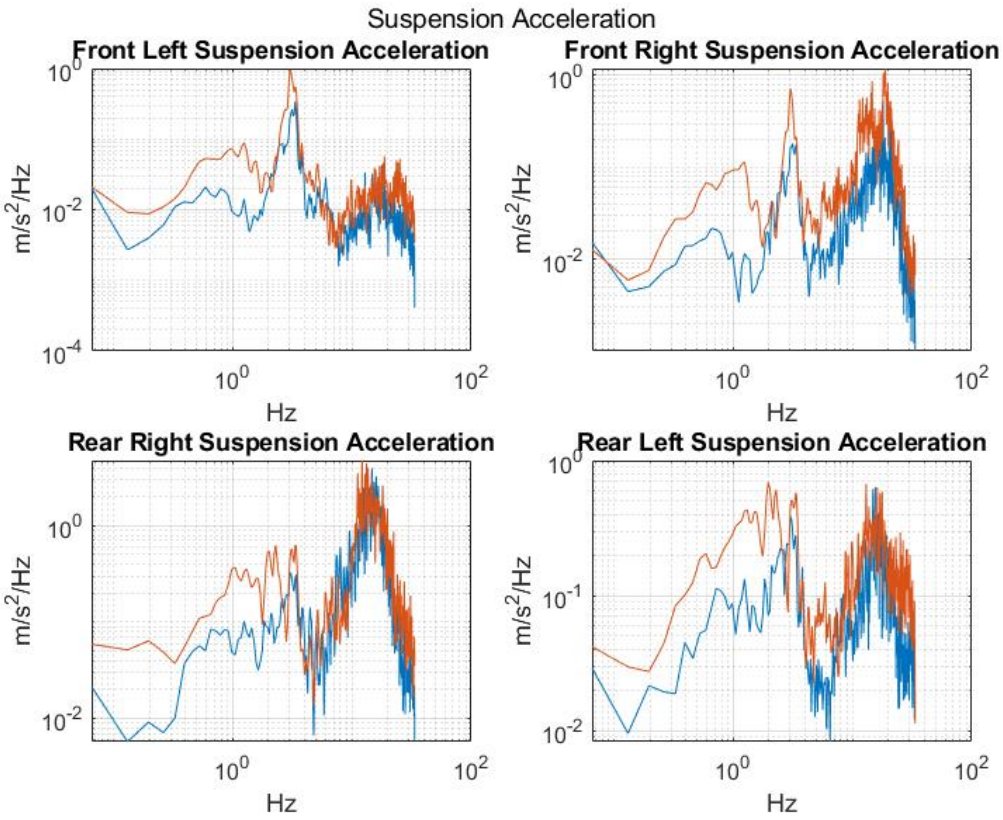

Figure 4.17: Vertical suspension acceleration

In a similar fashion to the speed comparison on asphalt between the four suspenders, the two velocities produce similar signals with some difference in power content. The difference is most prevalent in the front right suspender.

The next plots in figure 4.18 contains the data for the left front spindle and feather tower accelerometers.

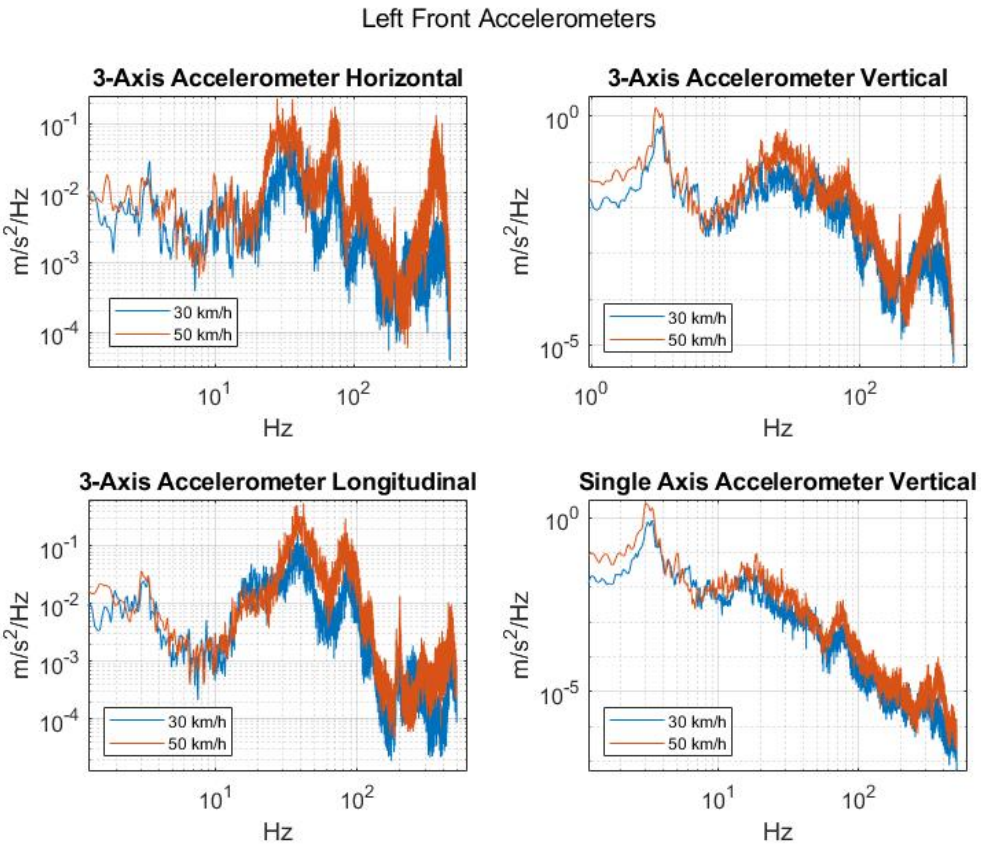

Figure 4.18: Left front accelerometers

In the front left three-axis accelerometers there is a distinction in power content between the signals in the regions between 15-220 Hz and 260-500 Hz. A similar distinction in the single-axis accelerometer is present but the two signals of the velocities converge in the domain between 225-300 Hz.

Figure 4.19 shows the right front spindle and feather tower accelerometer.

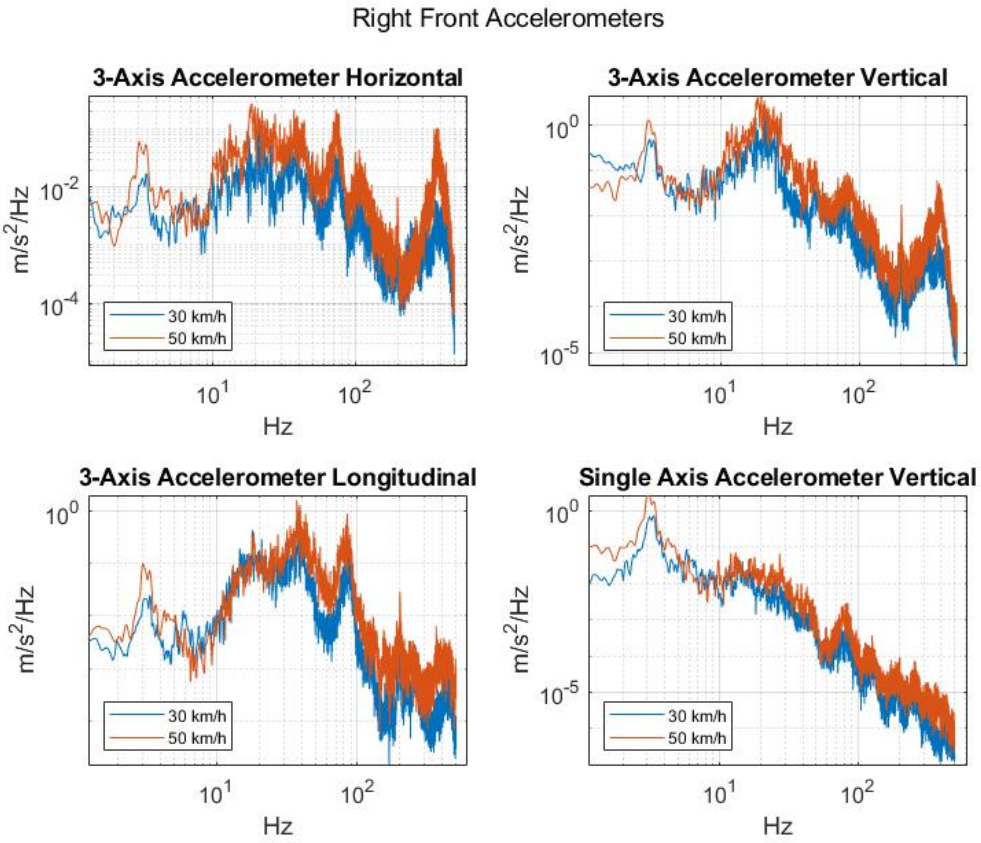

Figure 4.19: Right front accelerometers

The right front accelerometers portray very much the same picture as the left front accelerometers.

Figure 4.20 shows the left rear spindle and trunk accelerometer.

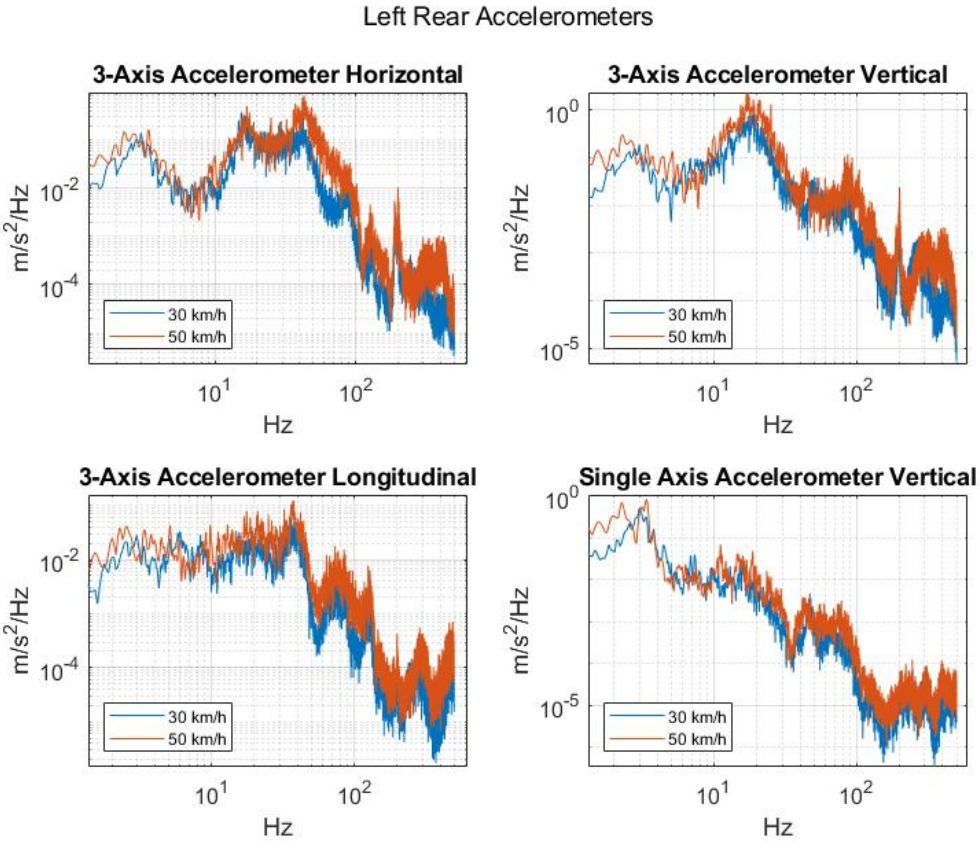

Figure 4.20: Left rear accelerometers

The difference in power content of the signals for the two speeds can be seen here in a similar manner to the plots previously presented in this section.

Figure 4.21 shows the right rear spindle and trunk accelerometer.

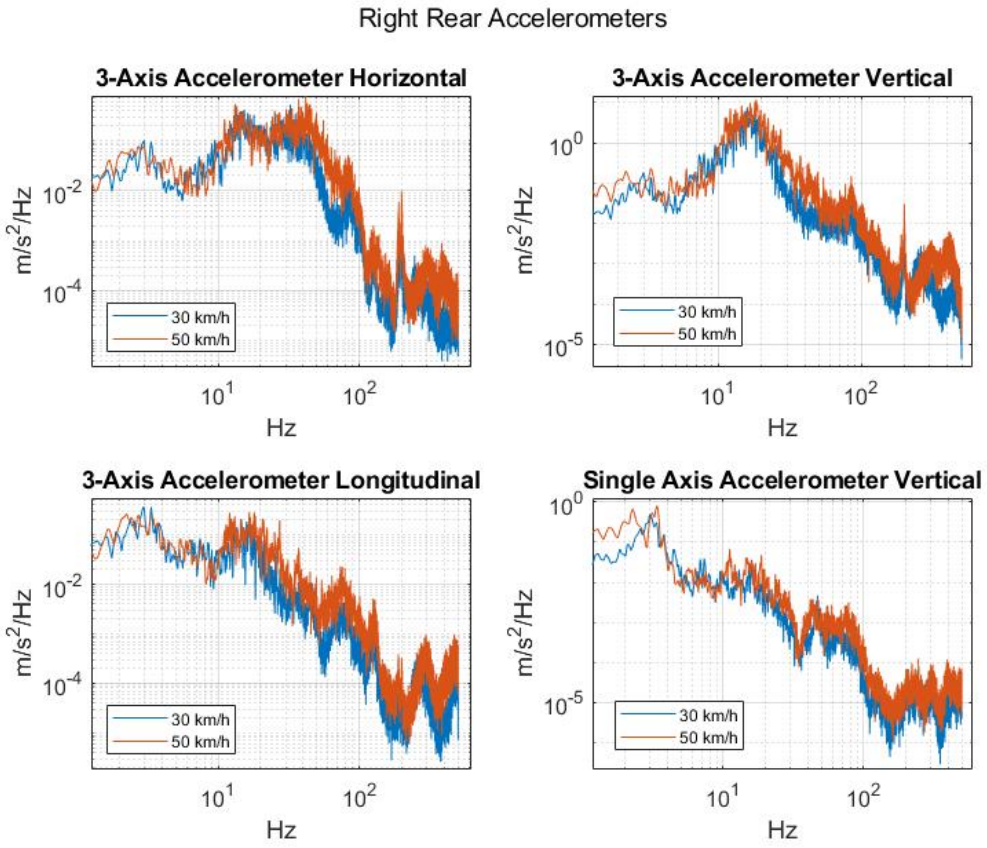

Figure 4.21: Right rear accelerometers

The right rear accelerometers show a high resemblance to the left rear accelerometers.

From the analysis it can be concluded that the velocity does affect the data acquisition. In all plots presented there are regions where the higher pace produces a signal with greater power content. This result seems logical as propelling a vehicle at a higher pace would create greater force between the car and the road. There are certain regions of frequency that are convergent between the two velocities for all accelerometers, there seems to be no region across the board that seems unaffected by difference in speed. The results suggest that there might be some merit to analysing a velocity normalised signal when estimating road surface.

4.4 Engine vibrations

The impact of the engine's vibrations were investigated to see how they affect the rest of the data.

In this data set the engine was slowly revved from idling speed at 875 rpm to 4000 rpm.

Below the four plots in figure 4.22 show how the vehicle's suspension was affected by the revving.

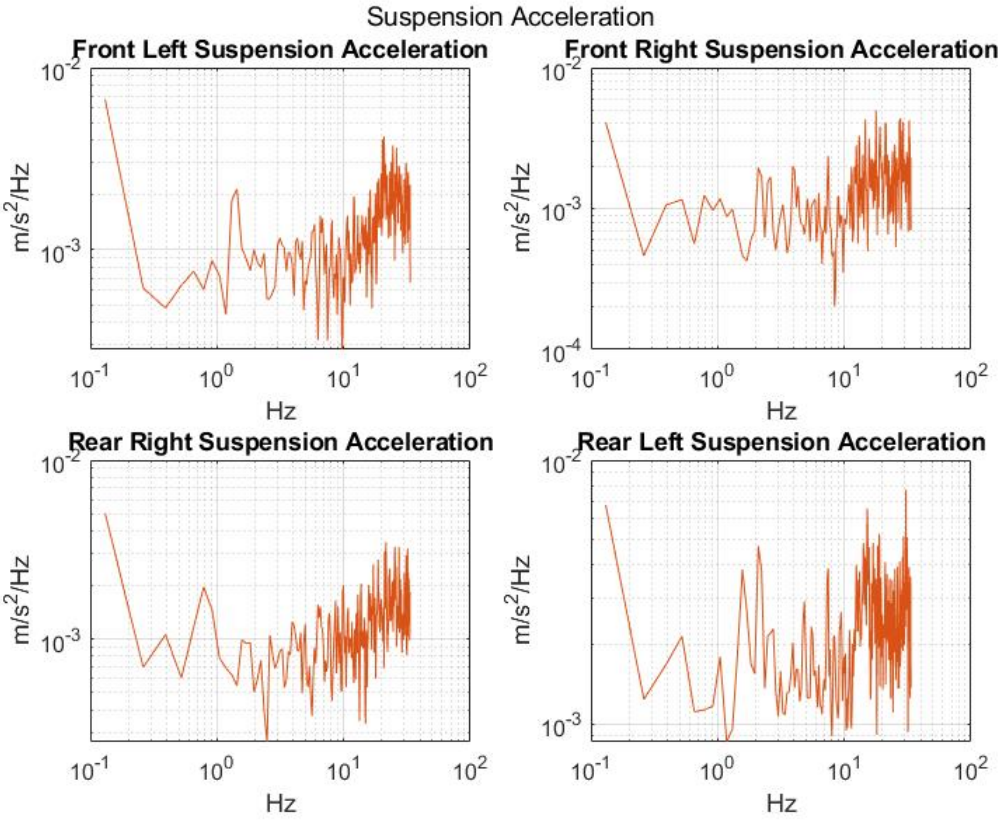

Figure 4.22: Vertical suspension acceleration

It can be seen in the four plots of the figure that most of the acceleration in the suspension occurs above 10 Hz. The front left, front right and rear right suspenders exhibit similar behaviour with the amplitude of the acceleration per Hz fluctuating between 10^{-3} and 10^{-2}. The signal of the rear left suspension has slightly higher power content than the other three signals.

In figure 4.23 the left front spindle and feather tower accelerometer.

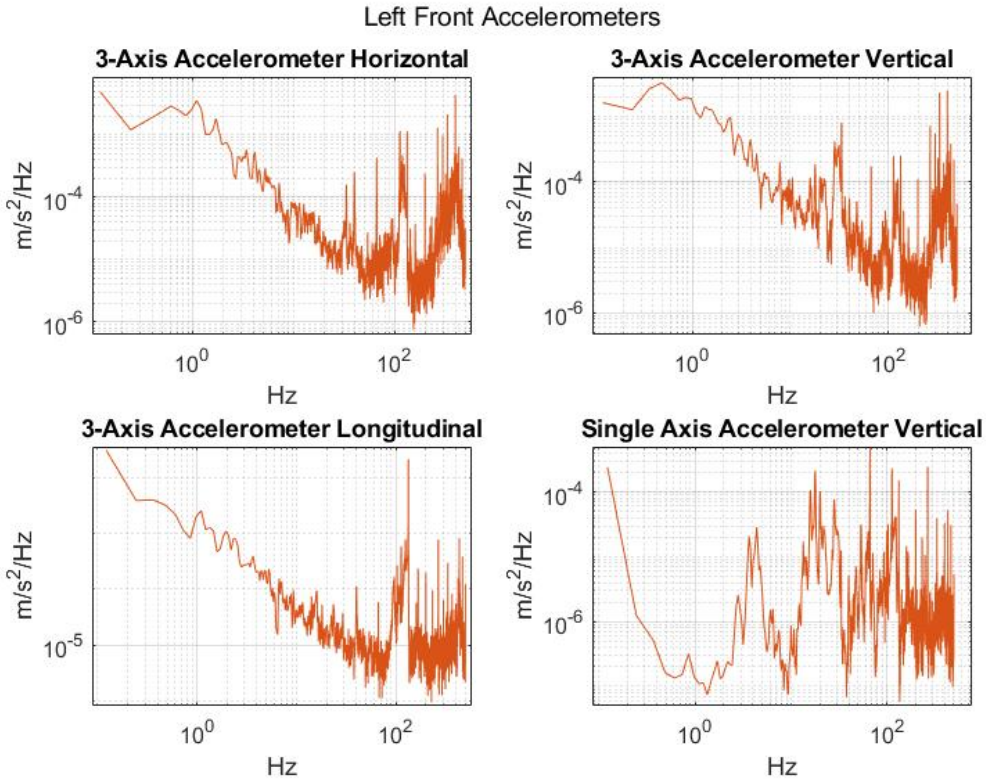

Figure 4.23: Left Front accelerometers

In the mounted accelerometers we can see that the power content of the signal is more evenly distributed as compared to the signals produced by the acceleration of the suspenders acquired from the CAN-bus. The horizontal and vertical axes of the accelerometer show similar behaviour with local maximas around 40, 80, 120, and 300-400 Hz. Even though it is more evenly distributed around than the previous graph, most of the acceleration occurs at higher frequencies. The power content of the signal is slightly lower overall compared to the suspension acceleration. The longitudinal acceleration has a local maxima at 120Hz and overall lower power content than the horizontal and vertical axes centered around 10^{-5} with prevalent local maximas around 100Hz and . The single-axis accelerometer has the lowest power content fluctuating around 10^{-6}.

Figure 4.24 shows the right front spindle and feather tower accelerometer.

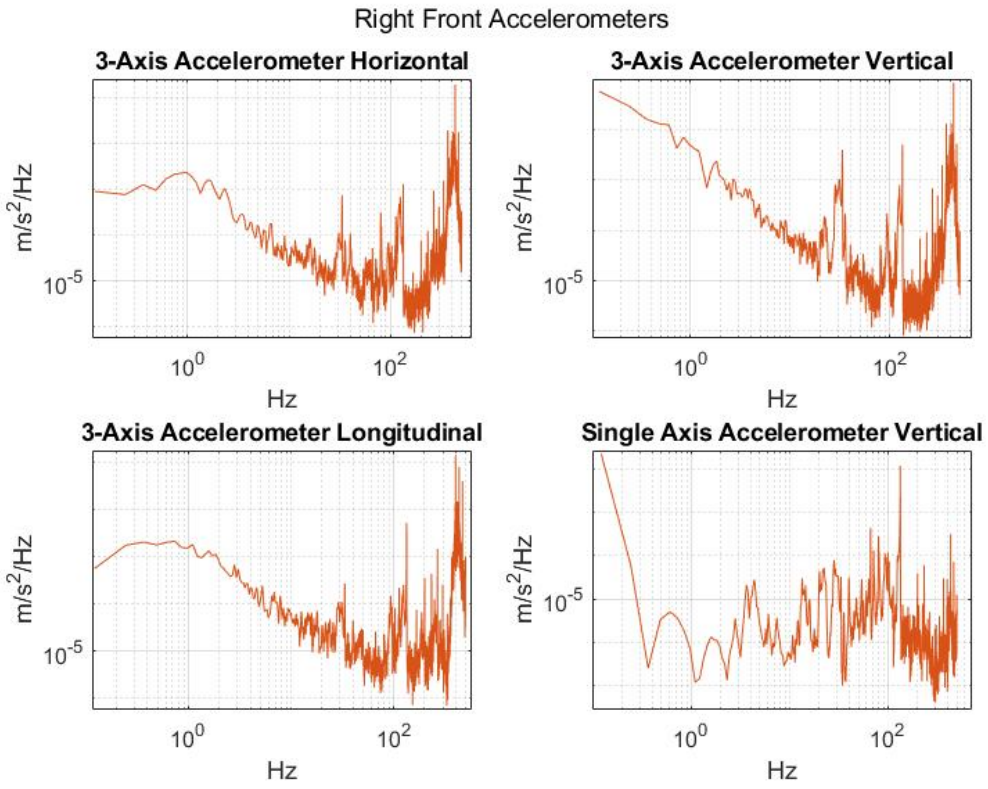

Figure 4.24: Right Front accelerometers

The right front accelerometers portray similarities with the left front accelerometers, although the longitudinal axis resembles the horizontal and vertical more in this cluster of plots as compared to the previous cluster. The single-axis accelerometer also resembles the one shown in the previous figure.

Figure 4.25 shows the left rear spindle and trunk accelerometer.

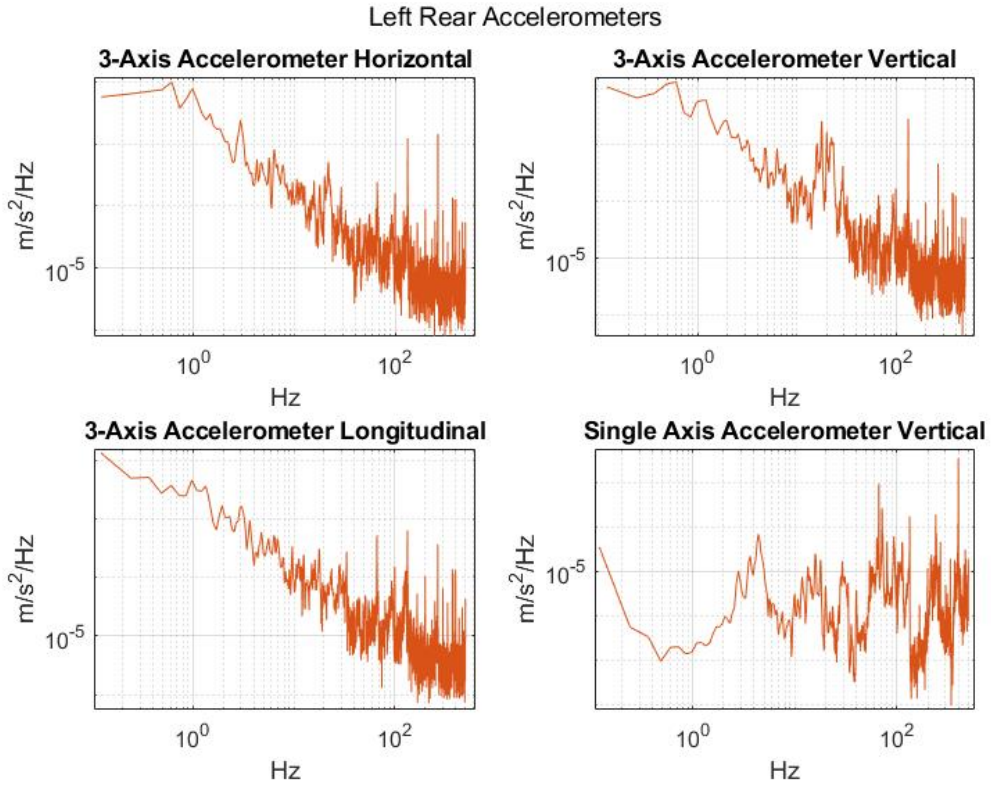

Figure 4.25: Left rear accelerometers

The left rear accelerometer shows an overall lower acceleration than the front mounted ones, while the single-axis accelerometer is much like the ones mounted in the front. A trend can be identified in the three-axis accelerometer where there almost is a linear decline in power content of the signal as the frequency increases.

Figure 4.26 shows the right rear spindle and trunk accelerometer.

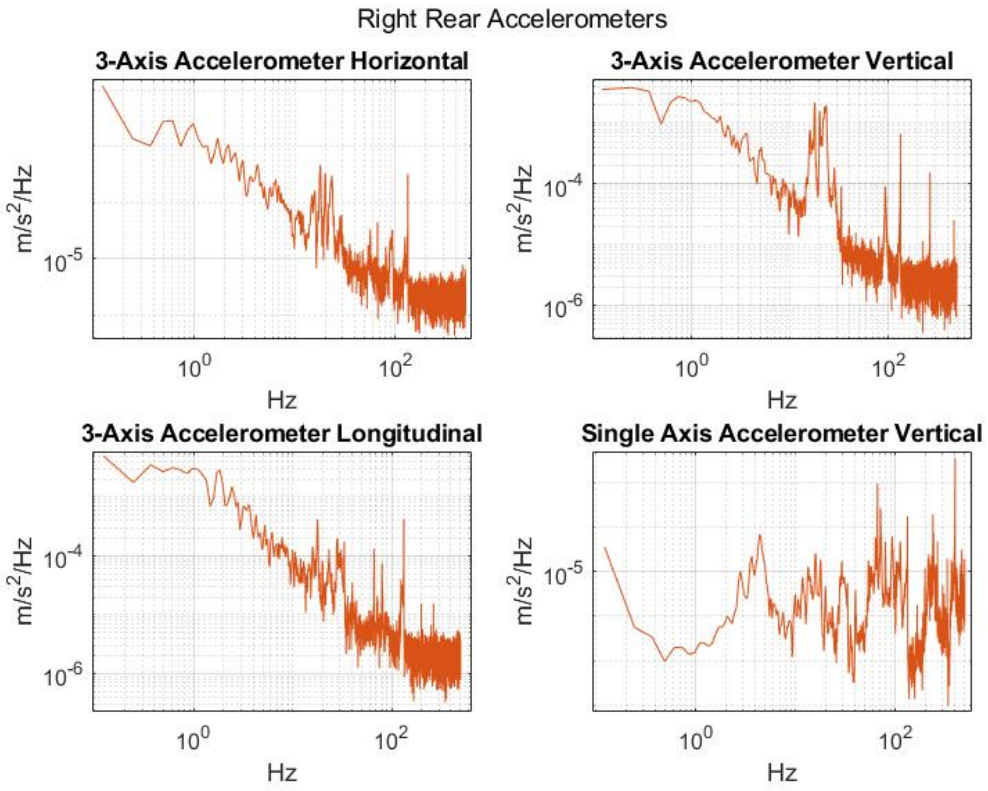

Figure 4.26: Right rear accelerometers

High resemblance to the left rear accelerometer figure previously presented although there is a local maxima around 15Hz. The single-axis accelerometer is the same as the foregoing plot and is included here to better portray the differences between the three-axis versus single-axis accelerometer.

Overall a few conclusions could be made:

- The motor vibrations were less prevalent in the single-axis accelerometers and occurred more frequently at above 100Hz.
- The motor vibrations were consistent in the three single-axis accelerometers.
- There is less vibration in the rear three-axis accelerometers than the front ones.

Overall it is shown that the vibrations do impact the measurements of the accelerometers to an extent greater than first expected.

The results suggest that higher frequencies are influenced by engine vibrations.

4.5 Comparing asphalt to gravel

In this portion of the thesis all the data acquired from the accelerometers and the CAN-bus will be analysed in order to determine which signal is the best at estimating road surface. It will also be investigated if there are any frequency domains that provide especially good indicators for the before mentioned purpose. The average velocity of the asphalt data was 59.2 km/h and 21.4 km/h for gravel.

4.5.1 single-axis accelerometers

First the single-axis accelerometers are to be examined. The very high coherence between the signals produced by these accelerometers previously presented in the coherence chapter suggests that only one of the three accelerometers need to be looked at. To establish this result further all three accelerometers are included in this comparison.

In figure 4.27 the left front single-axis accelerometer is shown.

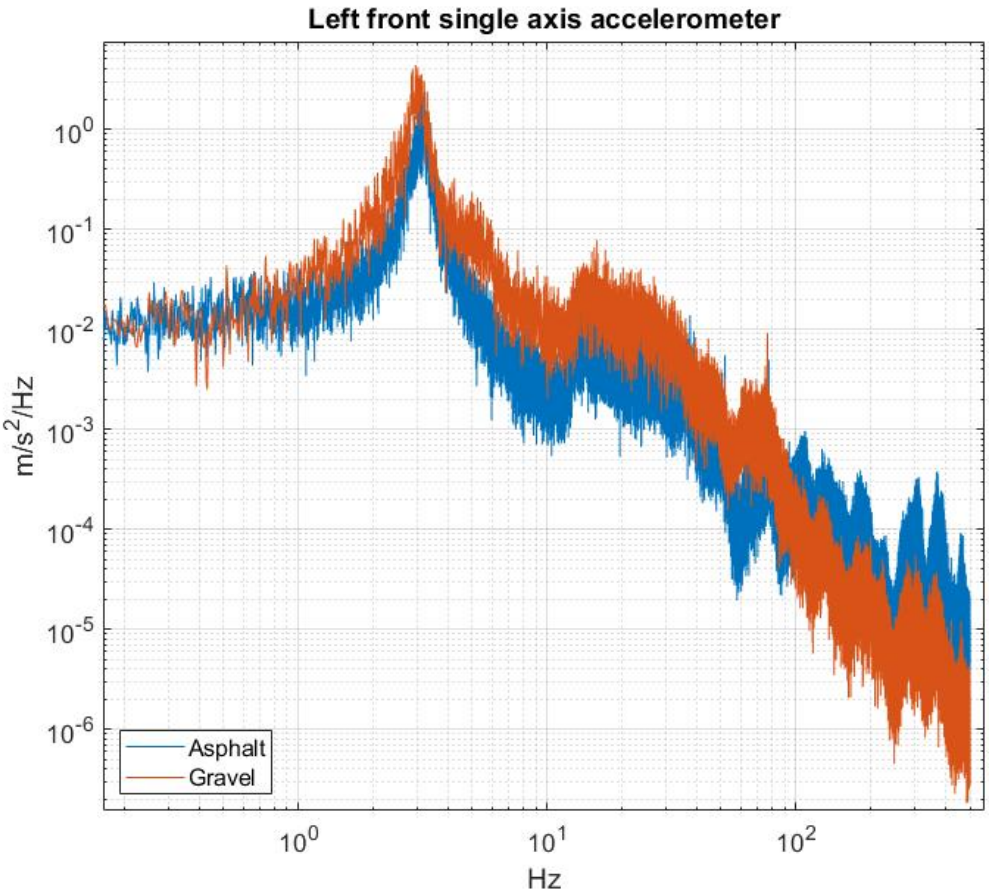

Figure 4.27: Left front single-axis accelerometer

Overall the power content of the gravel signal is higher than the asphalt one in the

region between 1 to 100 Hz. Above 100 Hz asphalt has higher power content than gravel.

The right front single-axis accelerometer is shown in figure 4.28.

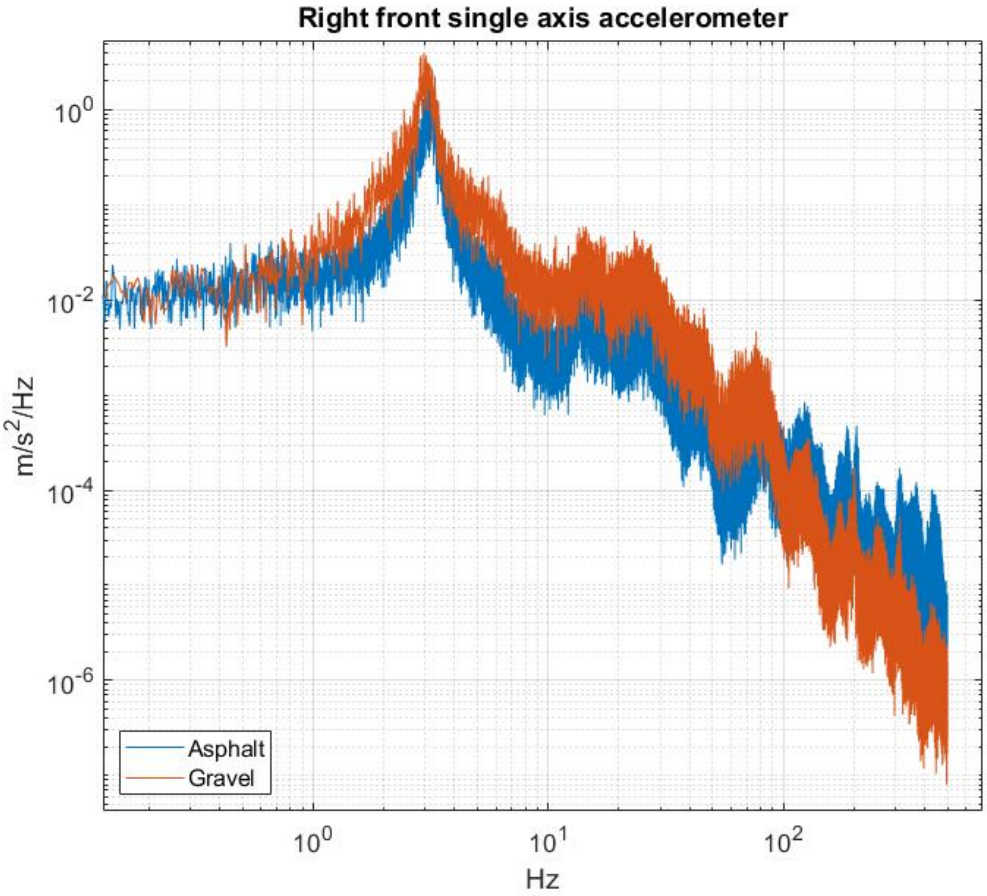

Figure 4.28: Right front single-axis accelerometer

In accordance with the findings in the coherence chapter the signals produced by this accelerometer are almost identical to the one produced by the left front single-axis accelerometer.

Figure 4.29 shows the single-axis accelerometer mounted in the trunk.

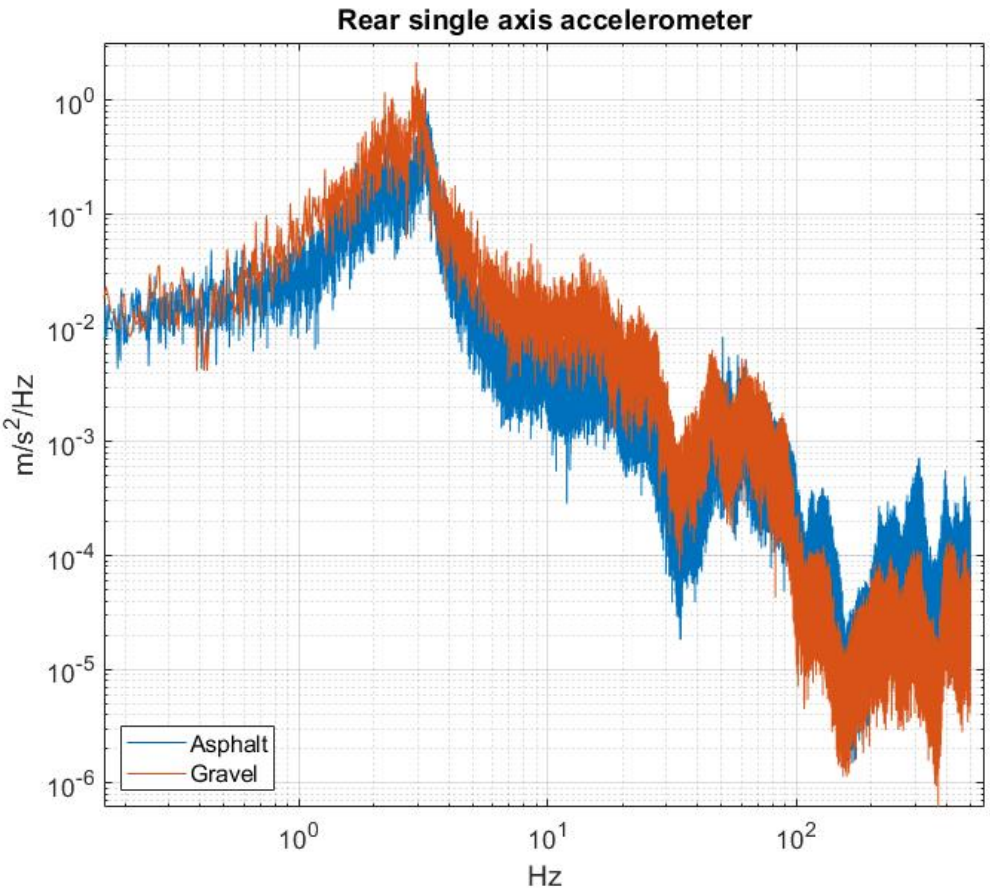

Figure 4.29: Rear single-axis accelerometer

There is a high resemblance to the other two single-axis accelerometers with similar frequency ranges of interest. Notably, the difference in power content between the two signals is lower as compared to the accelerometers mounted in the front.

In the engine vibration analysis it was suggested that the region above 100 Hz was influenced by the vibrations caused by the engine. The fact that all three plots presented in this section show higher power content for asphalt above 100 Hz suggest that the analysis in the engine vibration chapter is further established here. The average rpm for the asphalt data was 1843 rpm and 1382 rpm for gravel. Another factor for this can be the velocity but further tests need to be conducted in order to establish this.

4.5.2 Vehicle suspension acceleration

Next the four suspension accelerations from the CAN-bus are investigated.

In figure 4.30 the right front suspension accelerations is shown.

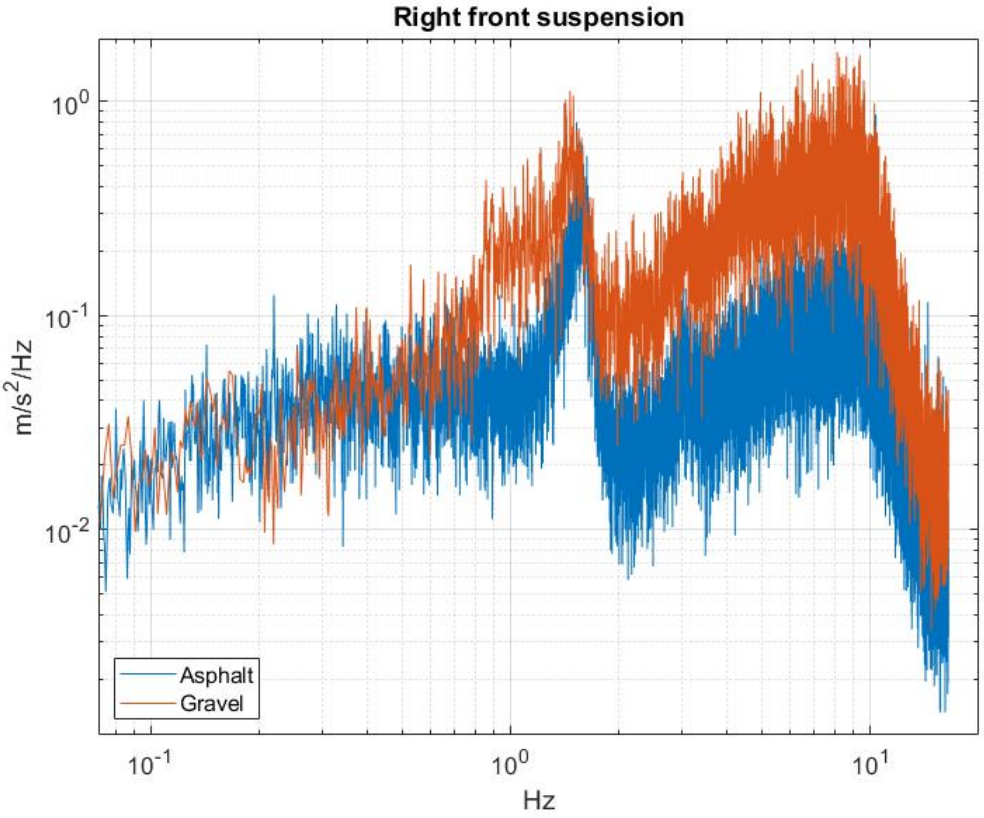

Figure 4.30: Right front suspension

There is a distinct difference in power content of the two signals, with gravel having greater power content.

Figure 4.31 shows the left front suspension accelerations.

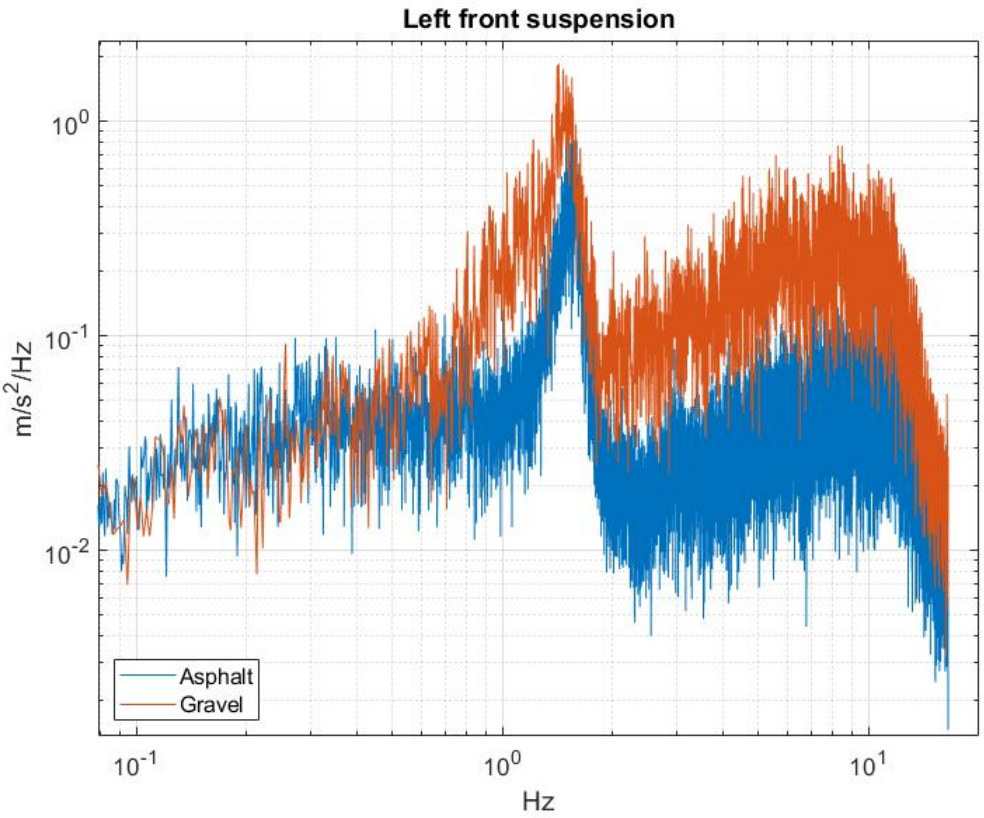

Figure 4.31: Left front suspension

Very similar to the right front suspension, and thus in accordance with the findings in the coherence analysis.

Right rear suspension acceleration is shown in figure 4.32.

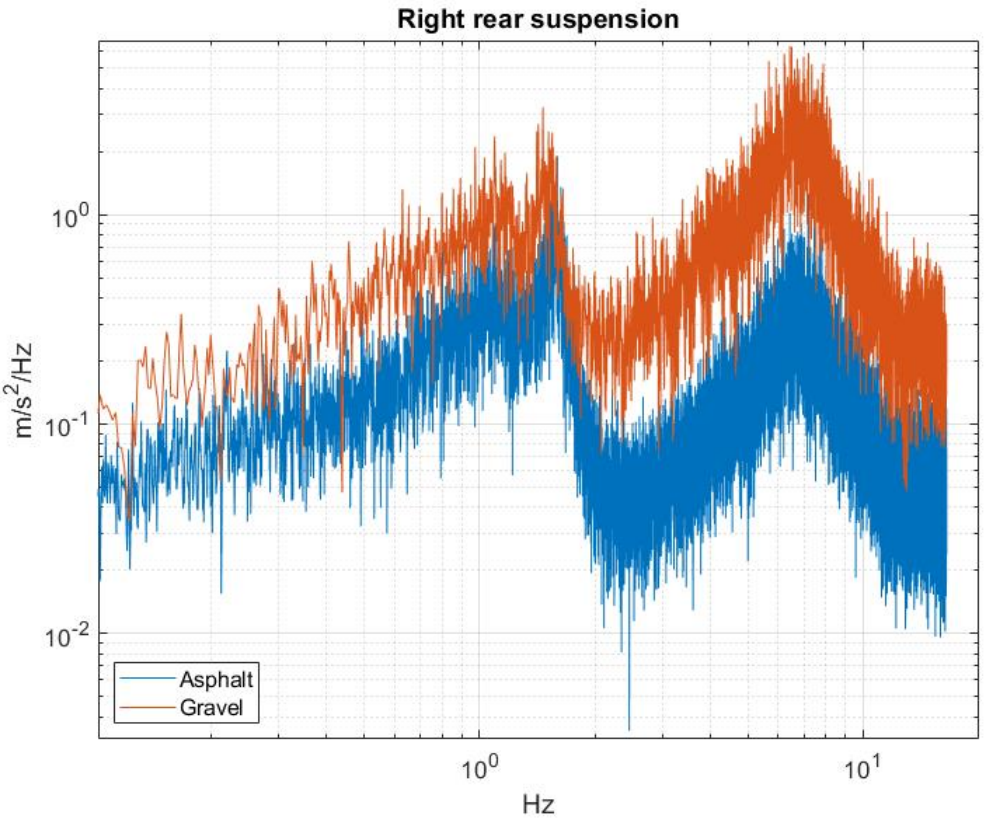

Figure 4.32: Right rear suspension

The right rear suspension shows an even greater difference in power content between the two signals as compared to the front suspension. Another thing worth mentioning is that the magnitude of the signals produced in this suspension is significantly higher than the ones in the front suspension.

Lastly in figure 4.33 the left rear suspension acceleration is shown.

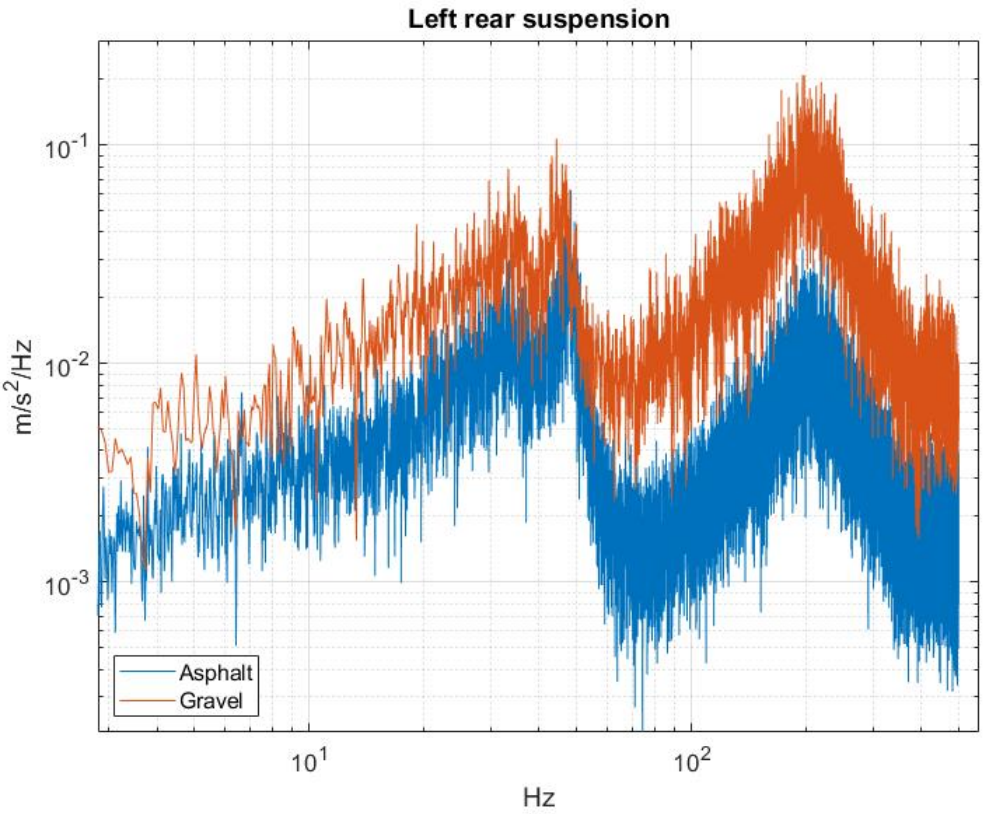

Figure 4.33: Left rear suspension

The left rear suspension produces a graph very similar to the right rear suspension.

In all the suspension data produce signals that seem very potent at distinguishing between asphalt and gravel. They appear to be unaffected by differences in engine vibrations and velocity.

4.5.3 Three-axis accelerometers

The final part in this analysis will focus on the three-axis accelerometers mounted on the spindles of the car.

Right front horizontal axes compared below in figure 4.34.

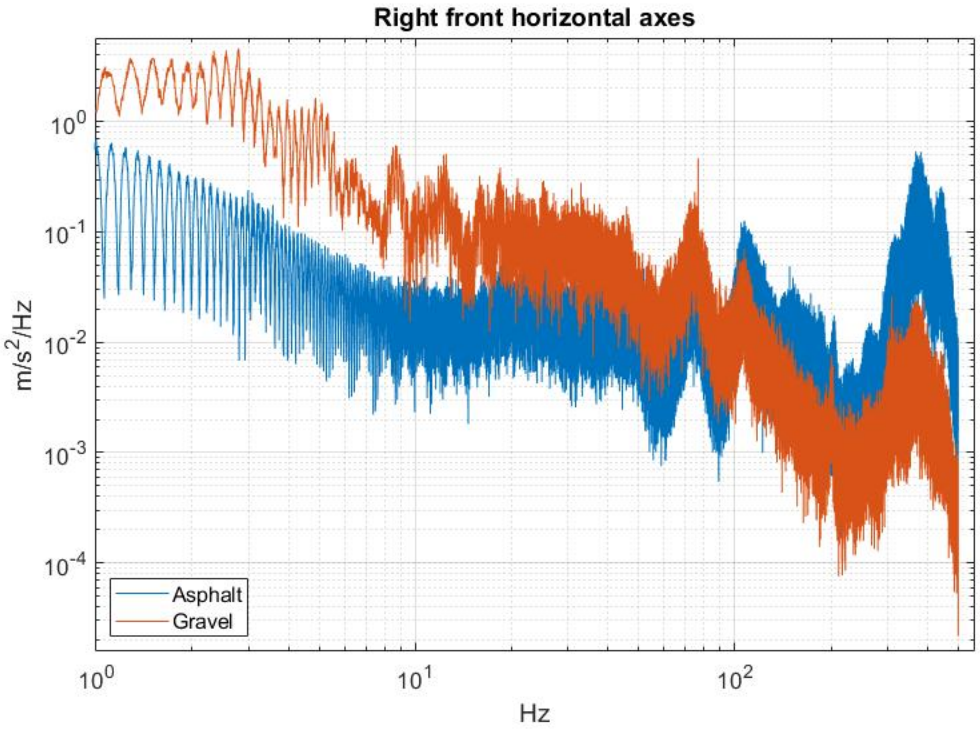

Figure 4.34: Right front horizontal axes

The right front horizontal axis shows very high power content in the region between 1 and 10 Hz. Furthermore, in the frequency domain between 1 to 100 Hz there is a difference in power content of the signals. In a similar fashion to the single-axis accelerometers the power content of asphalt is greater than that of gravel for frequencies above 100 Hz.

In figure 4.35 the right front vertical axes are compared.

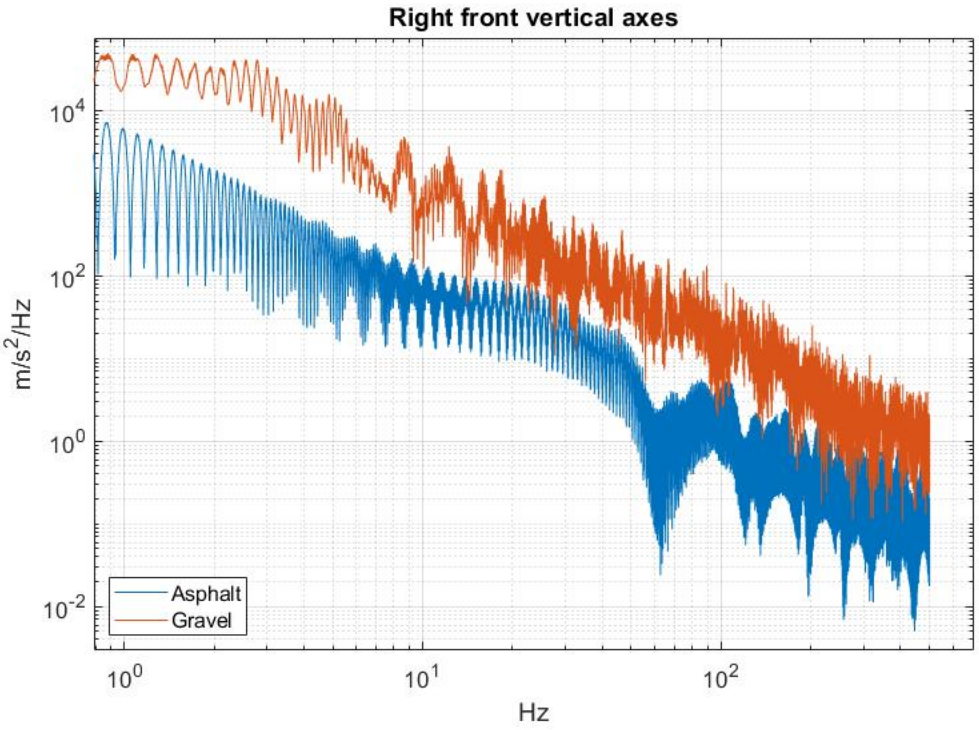

Figure 4.35: Right front vertical axes

The power content of the front vertical axes is immense. There is a clear distinction between the two signals in terms of power content across the whole frequency domain, with it becoming less prevalent above 200 Hz.

The right front longitudinal axes are compared in figure 4.36.

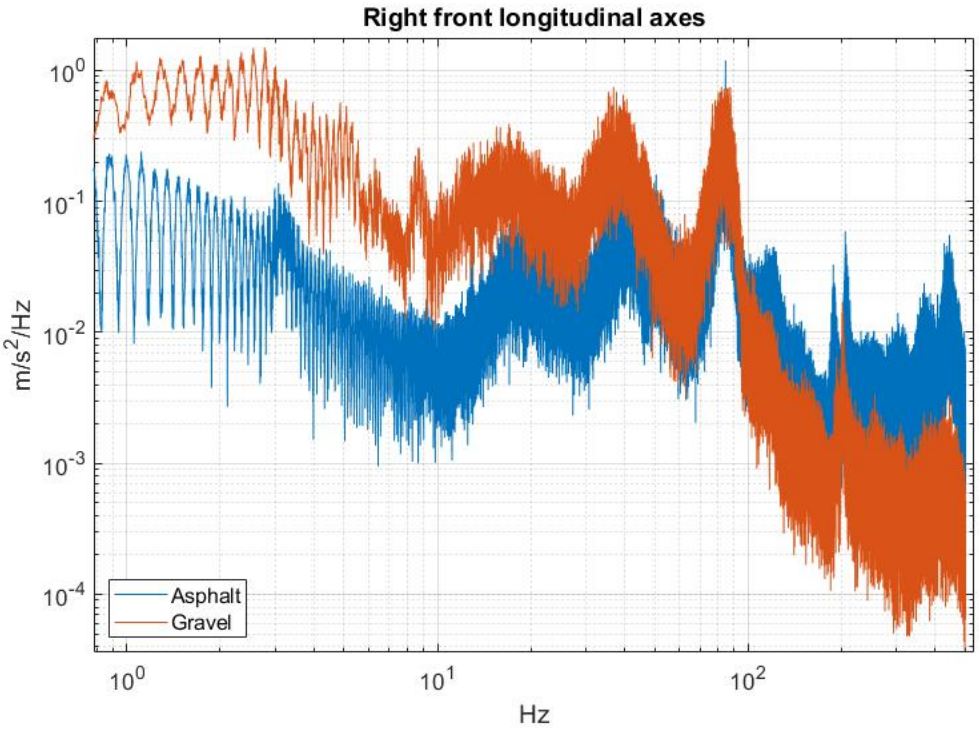

Figure 4.36: Right front longitudinal axes

Looking at the longitudinal axes there is a difference in power content of the signals in the region between 1 and 50 Hz. Same as for the horizontal axes, asphalt has a higher power content for frequencies above 100 Hz.

Figure 4.37 shows the left front horizontal axes.

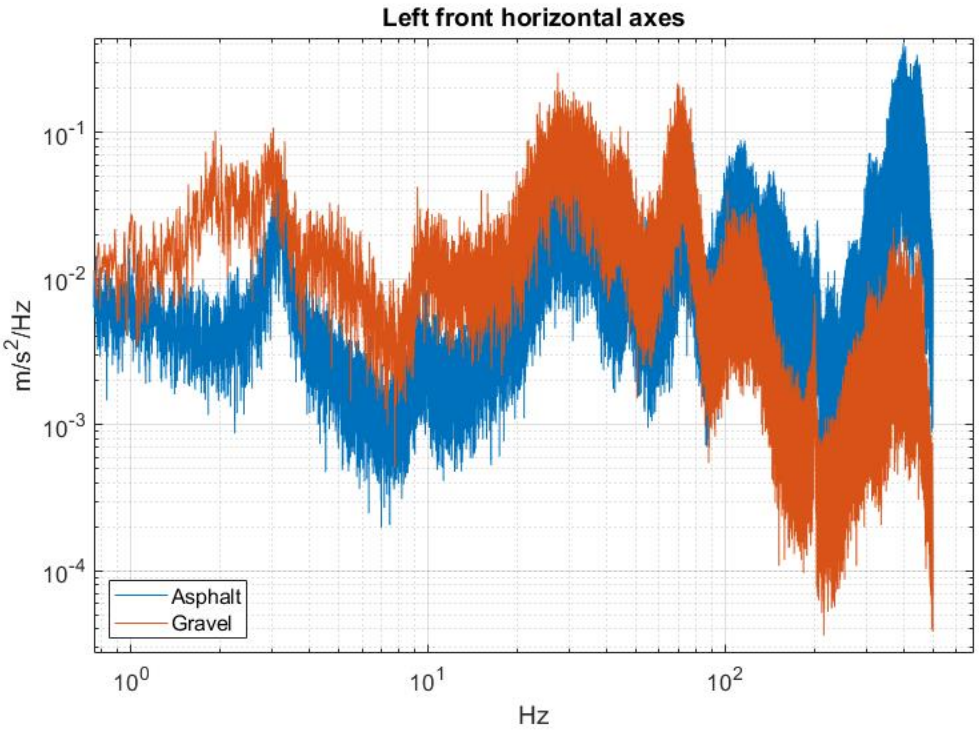

Figure 4.37: Left front horizontal axes

The region where gravel has higher power content than asphalt is located between 1 and 85 Hz. Above 100 Hz asphalt has higher power content. The overall magnitude of the signal's power contents is lower than the horizontal axes of the right front accelerometer.

The left front vertical axes are compared in figure 4.38 below.

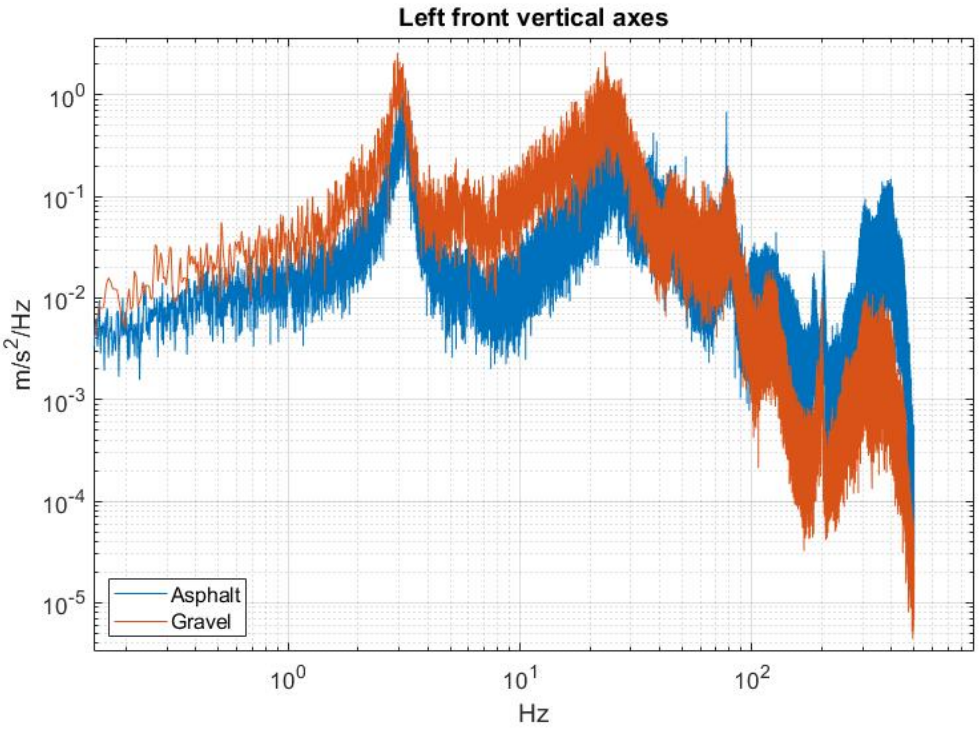

Figure 4.38: Left front vertical axes

In the same manner as the horizontal axes of the left front accelerometer the region 1 to 85 Hz gravel has a greater power content than asphalt. At frequencies above 100 Hz asphalt has the higher power content.

In figure 4.39 the left front longitudinal axes are compared.

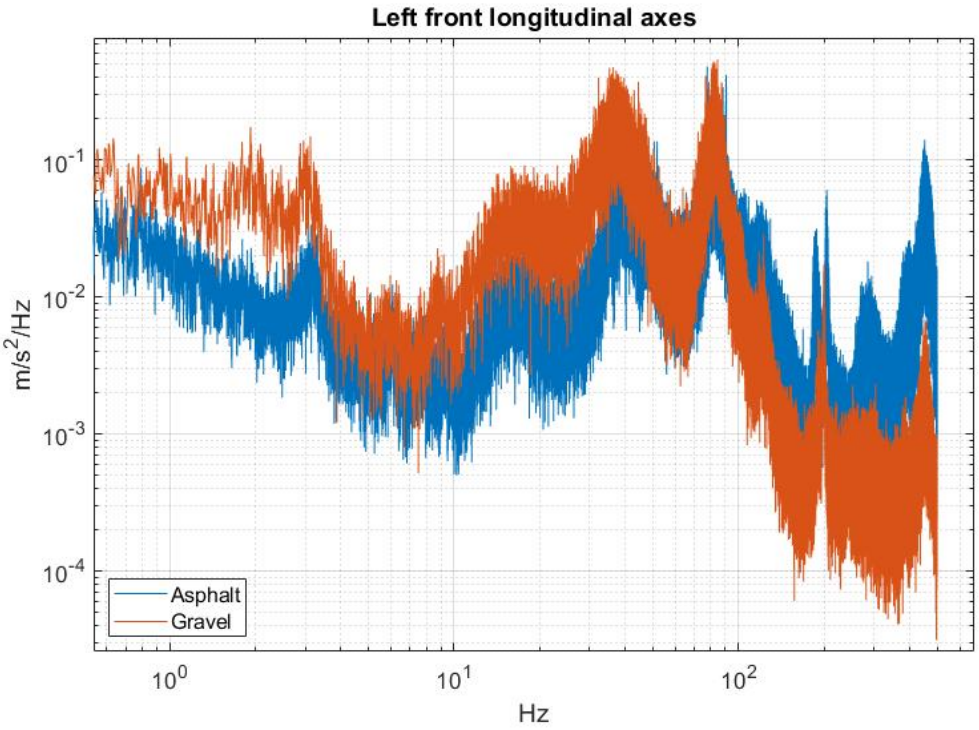

Figure 4.39: Left front longitudinal axes

The longitudinal axes are very similar to the horizontal axes.

Figure 4.40 shows the left rear horizontal axes.

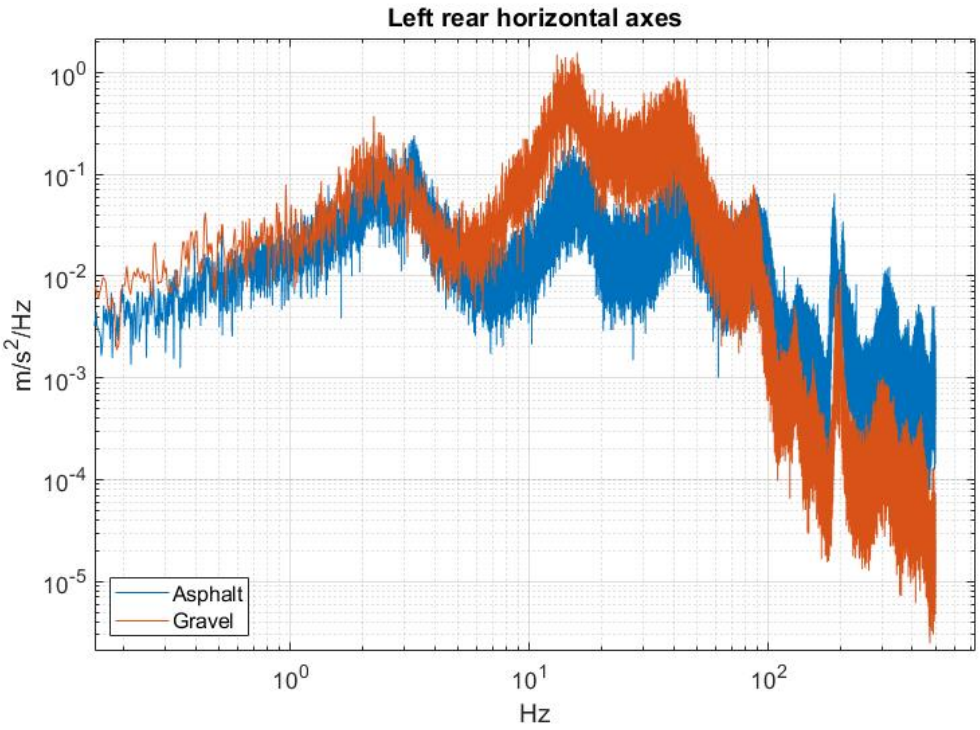

Figure 4.40: Left rear horizontal axes

For the left rear horizontal axes there is a clear difference in power content between the signals in the region 6 to 70 Hz with gravel being the highest. Above 100 Hz asphalt has greater power content.

The left rear vertical axes are compared in figure 4.41.

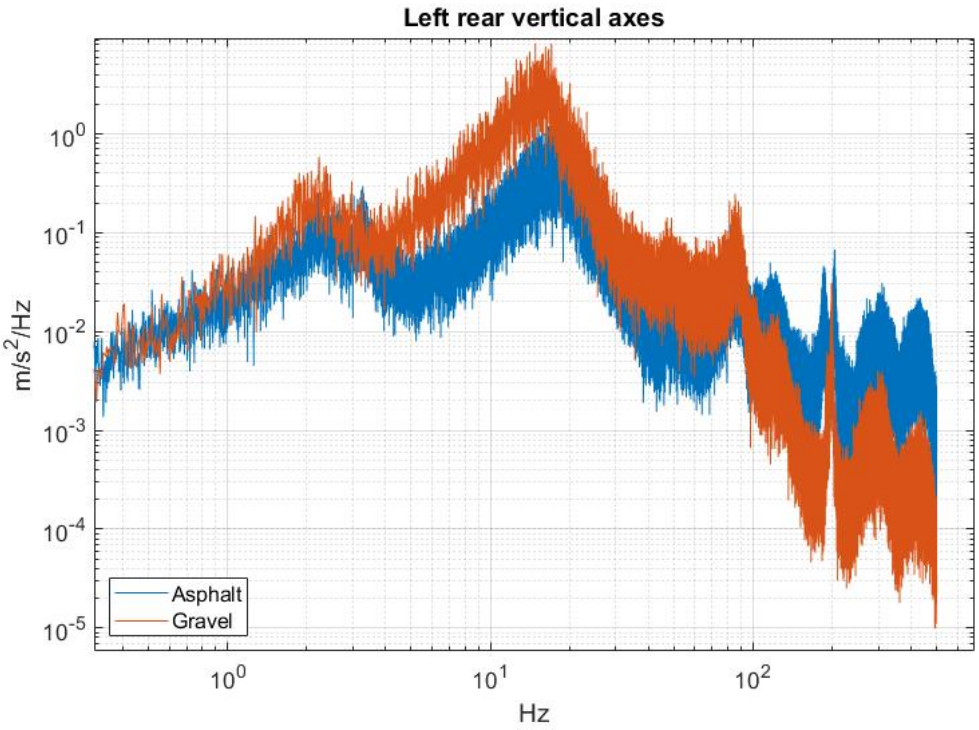

Figure 4.41: Left rear vertical axes

The left rear vertical axes show greater power content for the gravel signal between 1 to 90 Hz. Again above 100 Hz asphalt has higher power content.

Below figure 4.42 shows the left rear longitudinal axes.

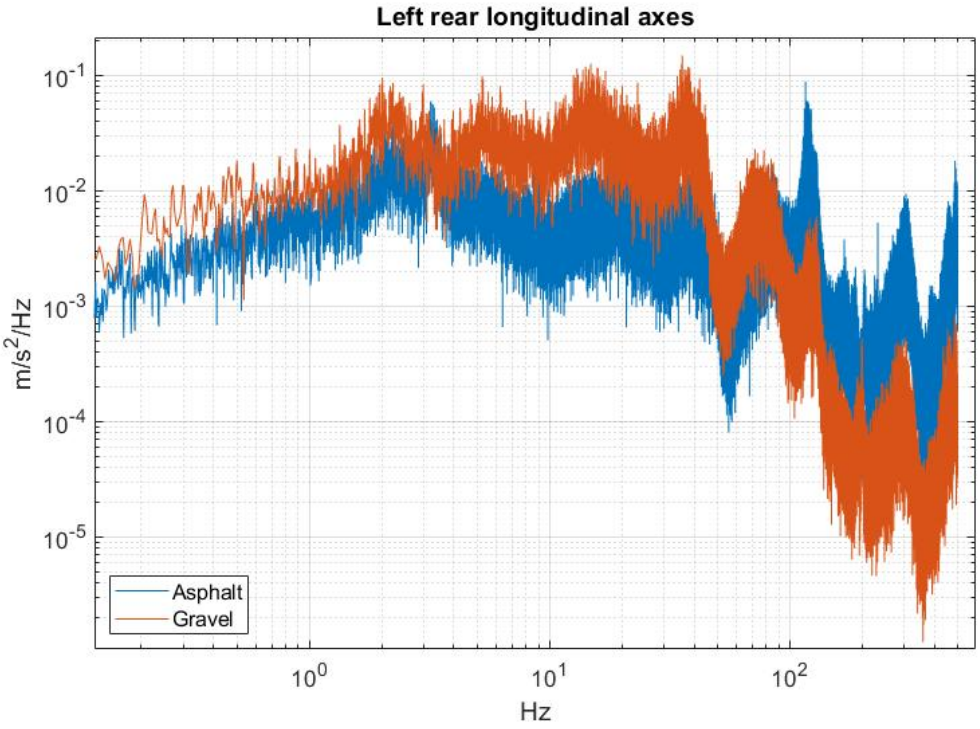

Figure 4.42: Left rear longitudinal axes

The longitudinal axes of the rear left accelerometer is very similar to the horizontal axes.

The right rear horizontal axes are compared below in figure 4.43.

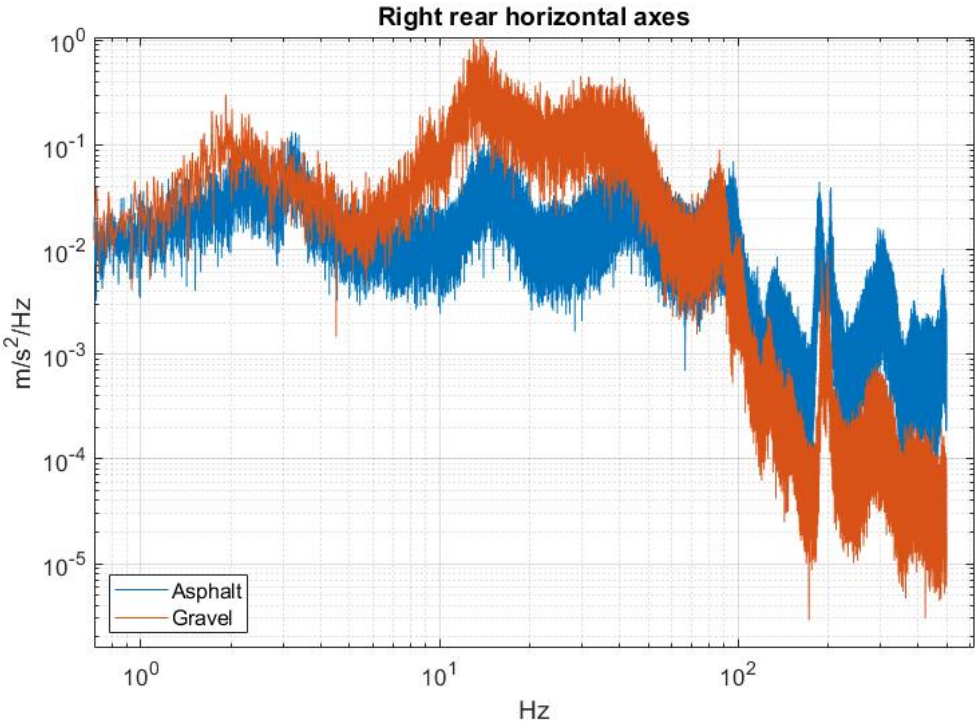

Figure 4.43: Right rear horizontal axes

The rear right horizontal axes are more or less identical to the rear left horizontal axes.

The right rear vertical axes are shown in figure 4.44.

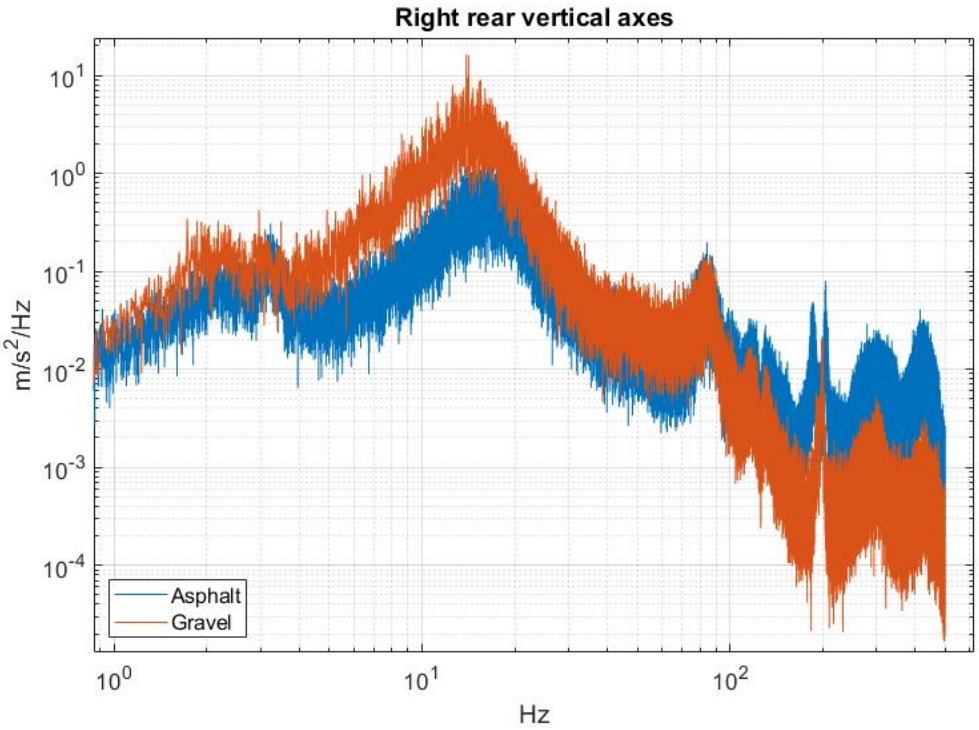

Figure 4.44: Right rear vertical axes

The right rear vertical axes are very similar to the left rear vertical axes.

Figure 4.45 shows the right rear longitudinal axes.

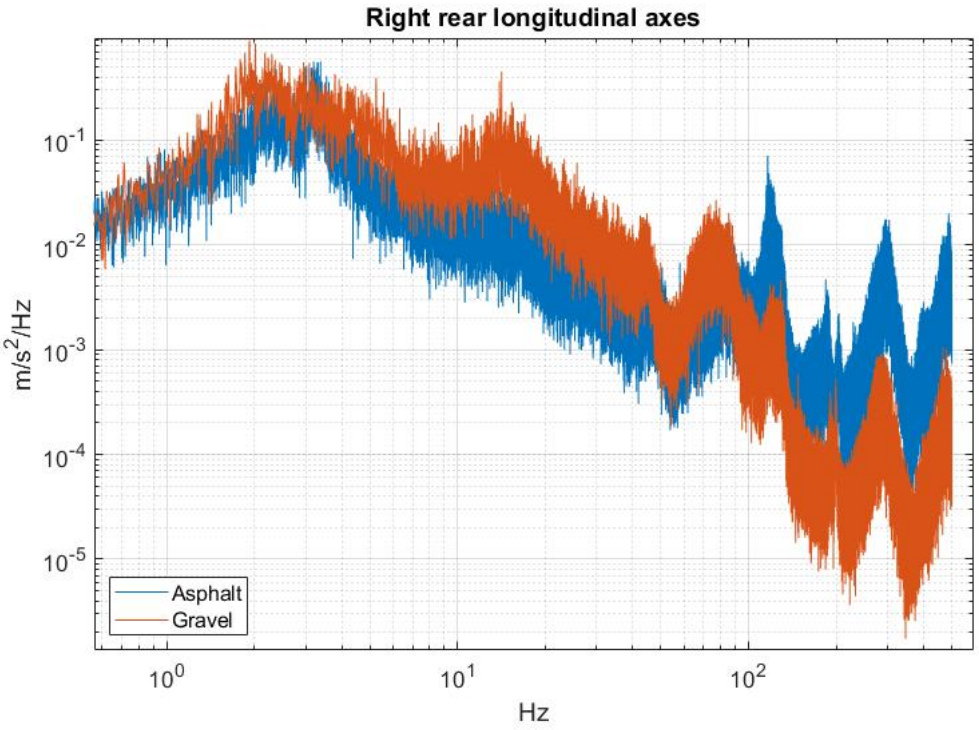

Figure 4.45: Right rear longitudinal axes

The rear right longitudinal axes gravel signal has greater power content in the region between 1 and 50 Hz. Above 100 Hz the asphalt signal has greater power content.

To summarize the three-axis accelerometer analysis at frequencies above 100 Hz asphalt has a higher power content and the reason why can be engine vibrations caused by the higher average rpm, but need to be investigated further to establish this as a fact.
An anomaly could also be detected. The power content of the front right accelerometer was significantly higher than any other signal. When reviewing the driving footage this was suspected to be due to a few factors: When driving on smaller roads facing oncoming traffic and pedestrians the car had to be driven as far right as possible and the surface was significantly rougher there. When driving the car on unknown roads a pothole could suddenly emerge and the initial impact on the front wheel would be greater than the rear wheel due to the fact that the driver would slow down when seeing or driving into the pothole thus hitting the front wheel harder than the rear wheel. The right front and back wheel was more frequently driven into potholes due to driver preference and a higher prevalence of potholes on the right hand side.
In all the signals produced by the three-axis accelerometers seem useful when estimating road surface. Although, the data suggest that they can be replaced by a single-axis accelerometer measuring force in the vertical direction.

5
Conclusion

5.1 Estimating road surface

The aim of this thesis was to estimate road surface in a reliable manner. The sheer number of factors to take into consideration were not apparent when the aim of the thesis was set. The measurements and analysis suggests that propelling a vehicle on gravel excitates the accelerometers more than driving on asphalt. However, this limited study does not establish this as a fact. This is due to the fact that a high quality gravel road can show the same result as a bad quality paved road. Furthermore, the data suggests that velocity and engine vibrations are factors that influence the data acquired. On top of that more extensive tests are needed.
However, some groundwork has been laid for further testing and analysis.

5.2 Presenting and interpreting data

During the analysis several ways of presenting data were attempted such as histograms, plotting the mean, raw plot of the acceleration data on a timeframe, power spectral density, and many others. With some trial and error, insight from our supervisor and a research department of Volvo, the best way to present the data was concluded to be Welch's power spectral density. As the power spectral density in combination with the averaging properties of Welch's method produces easily interpretable graphs with relevant information.

5.3 What signals are useful at estimating road surface

While we set out to estimate the road surface, the thesis ended up studying if the setup of the accelerometers mounted on the vehicle could be used for this purpose and which ones were the most effective at doing so. This, as aforementioned, because estimating the road surface is a very complex task.

5.3.1 Single-axis accelerometers

The coherence analysis in combination with the asphalt versus gravel analysis provides evidence that either of the three single-axis accelerometers mounted on the chassi can be useful when identifying road surface. Overall the difference between the measurements acquired with the three single-axis accelerometers are deemed negligible. Suggesting that only one chassi mounted accelerometer is enough.

The single-axis accelerometers seemed less affected by engine vibrations compared to the three-axis accelerometers, but more than the vehicle suspension. When analyzing the data with the help of Welch's power spectral density the domain between 1 to 100 Hz seemed to portray the roughness of the road quite accurately.The magnitude of the power content of the signal was overall less for the single-axis accelerometer as compared to the spindle mounted accelerometer and vehicle suspension acceleration.

5.3.2 Three-axis accelerometers

When investigating the three-axis accelerometers the high level of coherence between the internal axes indicates that they acquire the same data and that they can be replaced by a single-axis accelerometer. The vertical axis showed the highest power magnitude of the three axes and thus it seems fittest for acquiring data for the purpose of this thesis. Although, the horizontal and longitudinal axes seemed to be less affected by irregularities such as potholes for example.

When analysing the four different three-axis accelerometers there was a high amount of coherence between them as well, especially between the two rear ones. The two front ones seem to record spiky data with a lot of anomalies, especially when looking at smaller sets of data. Overall the rear ones seemed to produce stable, smoother data than the front ones, and it was concluded that the rear ones were less affected by engine vibrations and velocity differences.

The frequency region in which a difference in power content depending on the road surface can be seen varies between the different accelerometers and their axes but in general between 20 and 50 Hz gravel seems to produce a higher power content than asphalt.
The magnitude of the signals for the three-axis accelerometers were the highest of the data acquired. Above 400 Hz asphalt had higher power content than gravel which suggests something other than the vibrations caused by the road was being recorded as an uneven surface such as gravel should produce higher acceleration than asphalt.

5.3.3 Vehicle suspension acceleration

The coherence between the four suspenders of the vehicle was overall high and combined with the asphalt versus gravel analysis it can be concluded that recording data of only one suspender is enough. Even though the suspension data was collected much less frequently at 67Hz the sample rate was enough to draw the same conclusions as for the accelerometers that captured at 1 kHz.

Very noteworthy is that the suspension acceleration produces the most distinct difference in power content of the signals between asphalt and gravel. Also in comparison to the other accelerometers the suspension acceleration produced a signal for gravel with higher power content consistently above 1 Hz.

5.4 The most efficient signals for estimating road surface

While all accelerometers to some extent were able to distinguish between asphalt and gravel the rear vehicle suspension acceleration:

- Produces the most distinct difference in power content between the two surfaces.
- Were less affected by engine vibrations and difference in velocity.
- The lower sample rate still produces relevant data.

Thus, either of the rear two vehicle suspension accelerations are deemed fittest for this task by the merit of the reason mentioned above and the conducted analysis.

5.5 Going forward

To finalize this thesis a few suggestions can be made if anyone were to continue the investigation.

Looking at the results of this thesis from a condition monitoring point of view, attempting to estimate road surface perhaps is not the task which should be investigated. Knowing that the vehicle is traveling on gravel might not be useful information per se. As aforementioned a high quality graveled road can produce similar data to a paved road of poor quality. Exploring limiting factors of wear parts and connecting that with similar data acquired in this thesis is a suggestion.

While this thesis concluded that the rear vehicle suspension acceleration was the best at estimating road surface, more tests can be done to further establish this claim.

For example:

- Tests with controlled input instead of a random road.
- Tests on more different road types.
- More velocity trials.
- Influence of more extreme indices such as potholes, road bumps etc.
- Higher iteration tests in general.
- Trials with different vehicles.

Bibliography

[1] A. Raj, D. Krishna, HP. Ramachandran, KS. Singh, ND. Selvaraj, "Vision based road surface detection for automotive systems," in *2012 International Conference on Applied Electronics*, Pilsen, Czech Republic, 2012 [Online]. Available: `https://ieeexplore.ieee.org/abstract/document/6328908`, Accessed on: 2021-05-02.

[2] M. Yadav, B. Lohani, A.K. Singh, "ROAD SURFACE DETECTION FROM MOBILE LIDAR DATA," *ISPRS Annals of the Photogrammetry*, vol. IV-5, Nov, 2018. [Online]. Available: `https://pdfs.semanticscholar.org/ec6a/f2303088db8498b5d4f34c00a5d4e79b2634.pdf`, Accessed on: 2021-05-18.

[3] V. Astarita, M.V. Caruso, G. Danieli, D.C. Festa, V.P. Giofrè, T. Iuele, R. Vaiana, "A Mobile Application for Road Surface Quality Control: UNIquALroad," *Procedia - Social and Behavioral Sciences*, vol. 54, pp. 1135-1144, Oct, 2012. [Online]. Available: `https://www.sciencedirect.com/science/article/pii/S1877042812042905`, Accessed on: 2021-05-18.

[4] P.D. Welch, "The Use of Fast Fourier Transform for the Estimation of Power Spectra: A Method Based on Time Aver. aging Over Short, Modified Periodograms," *IEEE TRANSACTIONS ON AUDIO AND ELECTROACOUSTICS* vol. AU-15, nr. 2, ss. 70-73, Jun. 1967

[5] G.C. Carter, C.H. Knapp, A.H. Nutthall "Estimation of the Magnitude-Squared Coherence Function Via Overlapped Fast Fourier Transform Processin," *IEEE TRANSACTIONS ON AUDIO AND ELECTROACOUSTICS* vol. AU-21, nr. 4, ss. 337-344, Aug. 1973

DEPARTMENT OF MECHANICS AND MARITIME SCIENCES
CHALMERS UNIVERSITY OF TECHNOLOGY
Gothenburg, Sweden
www.chalmers.se

CHALMERS